Supersymmetric lattice fermions on the triangular lattice: superfrustration and criticality

2012 New J. Phys. 14 073002

(http://iopscience.iop.org/1367-2630/14/7/073002)

New Journal of Physics
The open-access journal for physics

Supersymmetric lattice fermions on the triangular lattice: superfrustration and criticality

L Huijse[1,7], D Mehta[2], N Moran[3,4], K Schoutens[5] and J Vala[4,6]

[1] Department of Physics, Harvard University, Cambridge, MA 02138, USA
[2] Physics Department, Syracuse University, Syracuse, NY 13244, USA
[3] Laboratoire Pierre Aigrain, ENS and CNRS, 24 rue Lhomond, 75005 Paris, France
[4] Department of Mathematical Physics, National University of Ireland, Maynooth, Ireland
[5] Institute for Theoretical Physics, University of Amsterdam, Science Park 904, PO Box 94485, 1090 GL Amsterdam, The Netherlands
[6] School of Theoretical Physics, Dublin Institute for Advanced Studies, 10 Burlington Road, Dublin 4, Ireland
E-mail: huijse@physics.harvard.edu

New Journal of Physics **14** (2012) 073002 (40pp)
Received 19 January 2012
Published 3 July 2012
Online at http://www.njp.org/
doi:10.1088/1367-2630/14/7/073002

Abstract. We study a model for itinerant, strongly interacting fermions where a judicious tuning of the interactions leads to a supersymmetric Hamiltonian. On the triangular lattice this model is known to exhibit a property called superfrustration, which is characterized by an extensive ground state entropy. Using a combination of numerical and analytical methods we study various ladder geometries obtained by imposing doubly periodic boundary conditions on the triangular lattice. We compare our results to various bounds on the ground state degeneracy obtained in the literature. For all systems we find that the number of ground states grows exponentially with system size. For two of the models that we study we obtain the exact number of ground states by solving the cohomology problem. For one of these, we find that via a sequence of mappings the entire spectrum can be understood. It exhibits a gapped phase at $1/4$ filling and a gapless phase at $1/6$ filling and phase separation at intermediate fillings. The gapless phase separates into an exponential number of sectors, where the continuum limit of each sector is described by a superconformal field theory.

[7] Author to whom any correspondence should be addressed.

Contents

1. Introduction

The supersymmetric model for lattice fermions was first introduced in [15] and has subsequently seen an intensive follow up in both the physics and mathematics literature (for a fairly recent overview see [19] and references therein). The key property of this model, namely supersymmetry, has the remarkable consequence that exact results can be obtained in the non-perturbative regime of a model for strongly interacting itinerant fermions.

These exact results have revealed a wide range of interesting phenomena in this system. On one-dimensional (1D) lattices one can typically find quantum criticality, which in combination with supersymmetry, gives rise to an effective continuum limit description in terms of a superconformal field theory [5, 13, 15, 20]. On general lattices the system furthermore exhibits a strong form of quantum charge frustration called superfrustration [14, 23, 36]. This property is characterized by an extensive ground state entropy. Other phenomena, such as edge modes, possible topological order and Rokhsar–Kivelson-like quantum liquid phases were also observed for this model [21, 22, 24]. Finally, a surprising connection between the supersymmetric model and the XYZ spin chain along a certain line of couplings has made it possible using supersymmetry to reinterpret some known properties and derive new results for the spin chain [11, 12, 18].

On the mathematics side, the study of supersymmetric lattice models has led to interesting results on the cohomology of independence complexes of lattices and graphs, 2D grids in particular [2, 4, 7–9, 16, 25–29]. The two sides are connected by the observation that quantum ground states of the supersymmetric lattice model are in one-to-one correspondence with the elements of the cohomology of an associated independence complex.

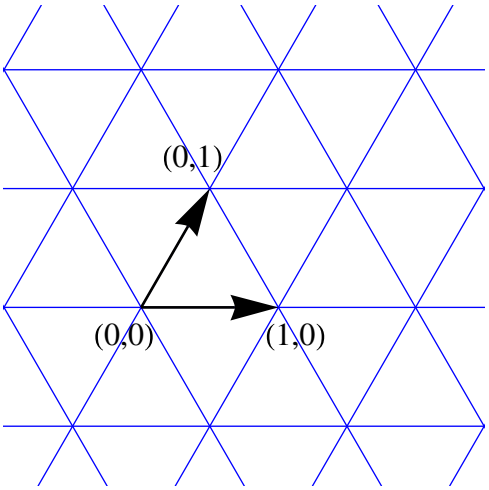

Figure 1. In this paper, we consider the supersymmetric model on the triangular lattice with doubly periodic boundary conditions. For the $M \times N$ triangular lattice the boundary conditions are imposed by requiring periodicity along two directions: $\vec{u} = (0, M)$ and $\vec{v} = (N, 0)$. The figure shows the two unit vectors along which the periodicities are imposed.

In this paper, we focus on the supersymmetric model on the triangular lattice. The ground state structure of this model is not fully understood. Various techniques that were successfully used to explore the ground state structure on other lattices have failed so far for this lattice. Nevertheless, a number of non-trivial results have been established for this model. The numerical computation of a lower bound on the number of ground states has shown that the system has an extensive ground state entropy [36]. Furthermore, analytic results on cohomology elements have revealed that degenerate quantum ground states occur in the entire range between $1/7$ and $1/5$ filling [29]. Finally, an upper bound on the number of quantum ground states was also obtained analytically [9].

In this work, we focus on ladder realizations of the triangular lattice by imposing doubly periodic boundary conditions (see figure 1). Using a combination of numerical and analytical techniques we study the ground state structure of these systems. We compare our results to the bounds that were previously established. For all systems we find that the number of ground states grows exponentially with system size. We numerically confirm that the range of filling for which zero energy states exist agrees with the range obtained by Jonsson. Furthermore, we prove analytically that there are no zero energy states outside the range between $1/8$ and $1/4$ filling. For two of the models that we study we obtain the exact number of ground states by solving the cohomology problem.

For the simplest ladder, the two-leg ladder, we uncover a symmetry that allows us to understand the origin of the exponential ground state degeneracy. This local $\mathbb{Z}_2$ symmetry distinguishes an exponential number of sectors. Subsequently, we present a mapping from the ladder to the chain such that the entire spectrum can be understood. Remarkably, in certain sectors the spectrum turns out to be gapped, in others it is gapless and in yet other sectors we find phase separation. The continuum limit of each of the gapless sectors is shown to be described by a superconformal field theory with central charge $c = 1$.

The paper is organized as follows. In the remainder of this section, we define the supersymmetric model, discuss the analytic and numerical techniques that we employ and, finally, summarize the results on the ground state degeneracy of the supersymmetric model on the triangular lattice that were established previously. In section 2, we present the numerical results we obtained for systems up to 54 sites and discuss how they relate to the known bounds and what they imply for the full 2D triangular lattice. In section 3, we focus on the three- and four-leg ladders, for which we obtain a number of analytical results on the ground state structure. Finally, in section 4 we present the full solution of the two-leg ladder.

1.1. The model

Supersymmetry is a symmetry between fermionic and bosonic degrees of freedom (see [3] for a general reference). It plays an important role in theoretical high energy physics, where various theories that go beyond the standard model require supersymmetry for a consistent formulation. In these theories, all the known elementary particles are accompanied by yet to be discovered superpartners.

In the lattice model discussed here the physical particles are spinless lattice fermions and the supersymmetry relates fermionic and bosonic many particle states with an odd and even number of the lattice fermions, respectively. In the $\mathcal{N} = 2$ supersymmetric theories that we consider, a central role is played by the operators Q and $Q^\dagger$, called supercharges, which have the following properties [37].

- Q adds one fermion to the system and $Q^\dagger$ takes out one fermion from the system.
- The supercharges are fermionic operators and thus nilpotent: $Q^2 = (Q^\dagger)^2 = 0$.
- The Hamiltonian is the anti-commutator of the supercharges, $H = \{Q, Q^\dagger\}$, and as a consequence it commutes with the supercharges and conserves the number of fermions in the system.

Imposing this structure has some immediate consequences: supersymmetric theories are characterized by a positive definite energy spectrum and a twofold degeneracy of each non-zero energy level. The two states with the same energy are called superpartners and are related by the supercharge.

From its definition it follows directly that H is positive definite:

$$\langle\psi|H|\psi\rangle = \langle\psi|(Q^\dagger Q + QQ^\dagger)|\psi\rangle$$

$$= |Q|\psi\rangle|^2 + |Q^\dagger|\psi\rangle|^2 \geqslant 0.$$

Furthermore, both Q and $Q^\dagger$ commute with the Hamiltonian, which gives rise to the twofold degeneracy in the energy spectrum. In other words, all eigenstates with an energy $E_s > 0$ form doublet representations of the supersymmetry algebra. A doublet consists of two states $(|s\rangle, Q|s\rangle)$, such that $Q^\dagger|s\rangle = 0$. Finally, all states with zero energy must be singlets: $Q|g\rangle = Q^\dagger|g\rangle = 0$ and conversely, all singlets must be zero energy states [37]. In addition to supersymmetry our models also have a fermion-number symmetry generated by the operator F with

$$[F, Q^\dagger] = -Q^\dagger \quad \text{and} \quad [F, Q] = Q. \tag{1.1}$$

Consequently, F commutes with the Hamiltonian. Furthermore, this tells us that superpartners differ in their fermion number by one (let $F|s\rangle = f_s|s\rangle$, then $F(Q|s\rangle) = Q(F+1)|s\rangle = (f_s+1)(Q|s\rangle)$).

An important issue is whether or not supersymmetric ground states at zero energy occur, that is, whether there are singlet representations of the algebra. For this one considers the Witten index

$$W = \mathrm{tr}\left[(-1)^F \mathrm{e}^{-\beta H}\right], \tag{1.2}$$

where the trace is over the entire Hilbert space. Remember that all excited states come in doublets with the same energy and differing in their fermion-number by one. This means that in the trace all contributions of excited states will cancel pairwise, and that the only states contributing are the zero energy ground states. We can thus evaluate W in the limit of $\beta \to 0$, where all states contribute $(-1)^F$. It also follows that $|W|$ is a lower bound to the number of zero energy ground states.

We now make things concrete and define a supersymmetric model for spinless fermions on a lattice, following [15]. The operator that creates a fermion on site i is written as $c_i^\dagger$ with $\{c_i^\dagger, c_j\} = \delta_{ij}$. To obtain a non-trivial Hamiltonian, we dress the fermion with a projection operator: $P_{\langle i\rangle} = \prod_{j \text{ next to } i}(1 - c_j^\dagger c_j)$, which requires all sites adjacent to site i to be empty. With $Q = \sum c_i^\dagger P_{\langle i\rangle}$ and $Q^\dagger = \sum c_i P_{\langle i\rangle}$, the Hamiltonian of these hard-core fermions reads

$$H = \{Q^\dagger, Q\} = \sum_i \sum_{j \text{ next to } i} P_{\langle i\rangle} c_i^\dagger c_j P_{\langle j\rangle} + \sum_i P_{\langle i\rangle}. \tag{1.3}$$

The first term is just a nearest-neighbor hopping term for hard-core fermions, the second term contains a next-nearest-neighbor repulsion, a chemical potential and a constant. The details of the latter terms will depend on the lattice we choose. In particular, for the triangular lattice we find

$$\sum_i P_{\langle i\rangle} = N - 6F + \sum_i V_{\langle i\rangle}, \tag{1.4}$$

where $V_{\langle i\rangle} + 1$ is the number of particles adjacent to site i.

The Hamiltonian describes spinless fermions with nearest-neighbor hopping and strong repulsive interactions. It is clear that supersymmetry requires fine-tuning of the parameters in the Hamiltonian. Nevertheless, there are physical systems that realize a similar type of interactions, such as ultra cold gasses of Rydberg atoms. The Van der Waals interaction between Rydberg atoms falls off as $1/r^6$, where r is the distance between two Rydberg atoms. It follows that the nearest-neighbor repulsion is almost two orders of magnitude larger than the next-nearest-neighbor repulsion. This results in what is called a Rydberg excitation blockade; atoms within a certain distance of a Rydberg atom cannot be excited to the Rydberg state. It follows that Rydberg atoms can be accurately modeled by itinerant hard-core fermions.

The hard-core constraint also arises naturally in dimer models. Dimer models were originally introduced to describe models of spin degrees of freedom with a strong preference to form spin singlets across links connecting neighboring spins. As a consequence, in these models the dimers are bosonic. More recently, however, fermionic dimer models have been discussed and, interestingly, a key feature of these models is a large ground state degeneracy [33, 34]. Possible relations between the supersymmetric model described here and fermionic dimer models were discussed in [22, 33, 34]. We find that a direct relation exists when we

introduce a staggering parameter in the supersymmetric model and study the extreme staggering limit. This limit strongly localizes the fermions and as a consequence the sign problem is reduced and can sometimes be fully gauged away to low orders in perturbation theory. For the supersymmetric model on the triangular lattice, however, no such techniques seem available and the system is believed to suffer from a full sign problem.

1.2. Methods

1.2.1. Cohomology techniques. For the supersymmetric models, cohomology has proven to be a very powerful tool to extract information about the zero energy ground state(s) of the models (see for example [14, 15, 19, 21, 25, 29] and references therein). The key ingredient is the fact that ground states are singlets; they are annihilated by both Q and $Q^\dagger$. This means that a ground state $|g\rangle$ is in the kernel of Q: $Q|g\rangle = 0$ and not in the image of Q, because if we could write $|g\rangle = Q|f\rangle$, then $(|f\rangle, |g\rangle)$, would be a doublet. So the ground states span a subspace $\mathcal{H}_Q$ of the Hilbert space $\mathbf{H}$ of states, such that $\mathcal{H}_Q = \ker Q/\mathrm{Im}Q$. This is precisely the definition of the cohomology of Q. So the ground states of a supersymmetric theory are in one-to-one correspondence with the cohomology of Q. It follows that the solution of the cohomology problem gives the number of zero energy states for each particle number sector. Equivalently, we find that zero energy states are in one-to-one correspondence with the homology elements of $Q^\dagger$.

We compute the cohomology using the 'tic-tac-toe' lemma of [6]. This says that under certain conditions, the cohomology $\mathcal{H}_Q$ for $Q = Q_1 + Q_2$ is the same as the cohomology of Q_1 acting on the cohomology of Q_2. In an equation, $\mathcal{H}_Q = \mathcal{H}_{Q_1}(\mathcal{H}_{Q_2}) \equiv \mathcal{H}_{12}$, where Q_1 and Q_2 act on different sublattices S_1 and S_2. We find $\mathcal{H}_{12}$ by first fixing the configuration on all sites of the sublattice S_1, and computing the cohomology $\mathcal{H}_{Q_2}$. Then one computes the cohomology of Q_1, acting not on the full space of states, but only on the classes in $\mathcal{H}_{Q_2}$. A sufficient condition for the lemma to hold is that all non-trivial elements of $\mathcal{H}_{12}$ have the same f_2 (the fermion-number on S_2).

Although ground states are in one-to-one correspondence with cohomology elements, the two are not equal unless the cohomology element happens to be a harmonic representative of the cohomology. Harmonic representatives are elements of both the cohomology of Q and the homology of $Q^\dagger$. So they are annihilated by both supercharges, which is precisely the property of a zero energy state. It follows that, although the solution of the cohomology problem gives the number of ground states, it typically does not give the ground states themselves. For a more leisurely introduction to cohomology and an exposition of the relation between the supersymmetric model and independence complexes we refer the reader to [19, 25].

We now briefly state the cohomology results for the 1D chain [15], because we will use these results many times throughout the paper. For the periodic chain of length $L = 3n + a$ the cohomology is trivial for all particle numbers, f, except for $f = n$, where we have

$$\dim(\mathcal{H}_Q) = \begin{cases} 1, & \text{for} \quad a = \pm 1, \\ 2, & \text{for} \quad a = 0. \end{cases} \tag{1.5}$$

Similarly, for open boundary conditions we have

$$\dim(\mathcal{H}_Q) = \begin{cases} 1, & \text{for} \quad \mathrm{a} = 0 \quad \text{and} \quad \mathrm{a} = -1, \\ 0, & \text{for} \quad \mathrm{a} = 1, \end{cases} \tag{1.6}$$

for a chain of length $L = 3n + a$ and n particles and $\dim(\mathcal{H}_Q) = 0$ at all other particle numbers. In particular, we note that the cohomology of an isolated site that can be both empty and occupied ($L = 1$ with open boundary conditions) is trivial. This is equivalent to the statement that the single site chain has no zero energy states, indeed the empty and occupied state form a doublet of energy $E = 1$.

1.2.2. Numerical methods. To complement the analytical techniques we also investigated a range of numerical methods. The goal of these techniques is to find accurately the number of degenerate zero energy eigenvalues of a given Hamiltonian. In principle there are many ways to compute this number. Here we describe some algebraic approaches we tried and also the iterative diagonalization method which was found to be the most effective.

1. *Characteristic polynomial*. Since the roots of the characteristic polynomial of a given matrix are the eigenvalues of the matrix, it is instructive to obtain the characteristic polynomial equation of the above Hamiltonian and solve it. However, the characteristic polynomial of a matrix bigger than 4×4 is a univariate of degree more than four, which is known to be exactly non-solvable in terms of the radicals of its coefficients as the Abel–Ruffini theorem states. This means that we have to rely on numerical methods to solve univariate polynomials for the Hamiltonians of sizes bigger than 4×4. Such numerical methods, e.g. Newton's method, are impractical because even small round-off errors in the coefficients of the characteristic polynomial can end up being a large error in the eigenvalues and hence in the eigenvectors.

   However, since in this specific problem we know that the ground state eigenvalue is exactly zero and we thus only need to compute its degeneracy, we may get away from the round-off error problem by only obtaining the characteristic polynomial and studying its structure. In particular, since we know that the lowest lying eigenvalues in our case are all degenerate eigenvalues, we can do the following: obtain the characteristic polynomial of the given Hamiltonian of size, say, N. Then, factorize the univariate polynomial (in the variable, say, x) such that the final form of the polynomial is $x^m(a_k x^k + \ldots + a_0 x^0)\ldots = 0$, where $m + k = N$. Here, m is now the number of the degenerate lowest lying eigenvalues. The problem here is that obtaining the characteristic polynomial itself is a quite extensive task as the matrix size increases. In particular, we could not easily go beyond the 4×6 triangular lattice (where the largest matrix dimension is 1188) on a single computer.

   Looking at the structure of the characteristic polynomial, we can also deduce that we may just need the smallest i in the characteristic polynomial written in the generic form as $\sum_{i=0}^{i=N} a_i x^i$ for which $a_i \neq 0$ since this i is m in the above notation, i.e. the number of degenerate lowest lying eigenvalues. However, again, since a_i is the sum over all the $i \times i$ minors of the matrix, the computation immediately blows up, restricting us again to the matrices of sizes as mentioned above.
2. *Rank of the matrix*. The rank r of a matrix of dimension N is less than N if there are $N - r$ zero modes. Since our Hamiltonian is known to have zero eigenvalues as the degenerate lowest lying eigenvalues, $N - r$ is the number of lowest lying eigenvalues in this case. This means that we just need to compute the rank of our Hamiltonian. However, the computation of the rank of a matrix is an extremely demanding calculation. We tried the singular value decomposition (the in-built routine of Matlab) and also computing the rank directly using various methods including the recently developed so-called numerical rank-revealing

method (with the RankRev package) [30, 31]. The latter method did perform slightly better than the singular value decomposition routine from Matlab. The method indeed correctly computes the number of degenerate eigenvalues, but scales exponentially with increasing matrix size and hence is not effective for even moderately sized lattices.

3. *Row–Echelon form*. Another way of computing the number of degenerate eigenvalues of a given matrix is to transform the matrix into Row–Echelon form and then to count the number of zero rows it has. Again, obtaining the Row–Echelon form of a matrix becomes a very difficult task since the number of steps in the algorithm increases exponentially with the dimension of the matrix. In particular, for the 4×4 lattice (matrix dimension of 96) this method completes successfully instantaneously (using Matlab's rref command), whereas already for the 4×6 lattice (matrix dimension 1188) this takes hours.
4. *Iterative diagonalization*. Here, we used the Krylov–Schur algorithm implementation from the SLEPc package [1] to compute the lowest lying eigenvalues. The DoQO [32] (Diagonalisation of Quantum Observables) toolkit was used to build the matrices and call the SLEPc routines. This method was chosen for its ability to resolve large numbers of degenerate states, which is not possible with the standard Lanczos algorithm. These methods scale linearly with the dimension of the matrix, but exponentially with the dimension of the degenerate subspace one is trying to resolve. In addition, unlike the techniques described above, it is not always guaranteed that all the degenerate zero energy states will be found. In particular, if the gap to the next excited state is too small or the dimension of the subspace within which the algorithm works is too small then the algorithm will not be able pick up all the zero energy degenerate states. The subspace can be increased but at the expense of exponentially more computational resources.

   In our calculations, we have taken steps to overcome these problems. Firstly, we exploit the symmetries of the Hamiltonian including particle conservation and space group symmetries to drastically reduce the dimension of the matrices involved and also the dimension of the degenerate zero energy subspace for each matrix. As well as this we check to ensure that the Witten index we compute matches that calculated via transfer matrix methods. This offers a very good check to ensure that we accurately account for all the zero energy ground states. Using these techniques we have been able to successfully calculate the numbers of degenerate ground states for triangular lattices with up to 54 sites (see appendix B), corresponding to the 6×9 triangular lattice (the full Hilbert space dimension here is on the order of 100 million. With filling and momentum conservation the largest matrix is on the order of 50 000).

In methods 1–3, we do not need to know the Witten index at all. But there the computation becomes heavy. Methods 1 and 3 can be used for the symbolic matrices too. So if there are some parameters involved in the Hamiltonian, for example, for the staggered matrices, we can still find the Row–Echelon form or the characteristic polynomial of the corresponding matrices. This is not the case for the purely numerical methods 2 and 4.

All in all, in our experiments with different methods, we conclude that the iterative diagonalization method scales better than any of the other methods we tried.

1.3. Summary of known results for the triangular lattice

In this section, we review results on the ground state structure of the supersymmetric model on the triangular lattice that were previously established. For further details we refer the reader to

the original publications. As mentioned in the introduction, a lower bound on the number of zero energy states was obtained in [36] by the numerical computation of the Witten index (1.2) for the $M \times N$ triangular lattice with periodic boundary conditions applied along two axes of the lattice. The numerical results immediately indicate an exponential growth of the absolute value of the Witten index. To quantify the growth behavior, the largest eigenvalue λ_N of the row-to-row transfer matrix for the Witten index on size $M \times N$ was determined. For the triangular lattice this gives [36]

$$|W_{M,N}| \sim (\lambda_N)^M + (\bar{\lambda}_N)^M, \quad \lambda_N \sim \lambda^N$$
$$|\lambda| \sim 1.14, \quad \arg(\lambda) \sim 0.18 \times \pi,$$

leading to a ground state entropy per site of

$$\frac{S_{\mathrm{GS}}}{MN} \geqslant \frac{1}{MN} \log |W_{M,N}| \sim \log |\lambda| \sim 0.13.$$

The argument of λ indicates that the asymptotic behavior of the index is dominated by configurations with filling fraction around $\nu = F/(MN) = 0.18$.

There are two main results for bounds on the total number of zero energy states for the triangular lattice. Both results were obtained by considering the (co)homology problem for the independence complex associated to the triangular lattice (see section 1.2.1). The first result, obtained by Jonsson [29], proves that zero energy ground states exist in a certain range of filling. He constructs a certain type of non-trivial homology element called cross-cycles. The size of a cross-cycle refers to the number of occupied sites in the homology element. If a cross-cycle of size k exists, it follows that the homology for k particles is non-vanishing. Using the relation between (co)homology elements and quantum ground states it follows that there exists at least one zero energy state with k particles. Jonsson obtains a bound on the size of the cross-cycles and this results in a bound on the particle numbers for which the homology is non-vanishing. That is, there is a set of rational numbers r, such that there exist cross-cycles of size rN, where N is the number of vertices of the 2D lattice. For the triangular lattice it is found that $r \in [\frac{1}{7}, \frac{1}{5}] \cap \mathbb{Q}$. In other words, there are zero energy ground states in the entire range between $1/7$ and $1/5$ filling.

Let us give the specific form of a cross-cycle z of size k.

- $z = \prod_{i=1}^{k} (|a_i\rangle - |b_i\rangle)$ such that z is a state in the Hilbert space with k particles, that is the a_i and b_i obey the hard-core condition.
- Furthermore, there is at least one configuration in z such that all sites in the lattice are either occupied or adjacent to at least one occupied site. This is called a maximal independent set.
- Finally, a_i is adjacent to b_i.

Note that, in this case, we consider the homology and not the cohomology. It is easily verified that z belongs to the kernel of $Q^\dagger$, since $Q^\dagger$ gives zero on each term in the product:

$$Q^\dagger(|a_i\rangle - |b_i\rangle) = |\emptyset\rangle - |\emptyset\rangle = 0.$$

The latter two conditions ensure that z is not in the image of $Q^\dagger$: the second condition ensures that there is no site c such that $Q^\dagger|c\rangle \prod_{i=1}^{k} (|a_i\rangle - |b_i\rangle) = z$ and the third condition ensures that $|a_j\rangle|b_j\rangle \prod_{i \neq j} (|a_i\rangle - |b_i\rangle)$ violates the hard-core condition.

Clearly, the latter two conditions, combined with the hard-core condition, impose certain bounds on the size of a cross-cycle. For the triangular lattice the size of the cross-cycles is at most a fifth of all the sites in the lattice and at least a seventh [29].

The second result that imposes a bound on the (co)homology on the triangular lattice was obtained by Engström [9]. He finds an upper bound to the total dimension of the cohomology for general graphs G using discrete Morse theory. He proves that if G is a graph and D a subset of its vertex set such that $G\backslash D$ is a forest, then $\sum_n \dim(\mathcal{H}_Q^{(n)}) \leqslant |\mathrm{Ind}(G[D])|$. Here $\mathcal{H}_Q^{(n)}$ is the cohomology of Q on the Hilbert space spanned by all hard-core particle configurations with n particles on the graph G and $\mathrm{Ind}(G[D])$ is the Hilbert space spanned by all hard-core particle configurations on the subset D. From this theorem it follows that finding the minimal set of vertices that should be removed from G to obtain a forest gives an upper bound on the total dimension of $\mathcal{H}_Q$ and thus on the total number of zero energy ground states for the supersymmetric model on the graph G. For the triangular lattice of size $2m \times n$ the upper bound was found to be approximately ϕ^{mn}, with $\phi = \frac{1}{2}(1+\sqrt{5})$, the golden ratio.

2. Results on ground states of the $M \times N$ triangular lattice

In this section, we discuss what we can learn about the ground state degeneracy on the triangular lattice in general from our numerical results. The total number of zero energy states in each particle number sector was computed numerically for lattices with up to 54 sites (see appendix B). We compare these results to the upper and lower bounds established by Engström and van Eerten, respectively. We also compare the fillings for which we found zero energy states to the bounds obtained by Jonsson.

Clearly, one has to be careful drawing conclusions for the full 2D triangular lattice from relatively small systems. We have decided to exclude the ladder geometries of size $2 \times L$ and $3 \times L$ in this analysis for the following reasons. First of all, in these geometries the particles cannot hop past each other due to the nearest-neighbor exclusion. One readily checks that the exclusion rule constraints the configurations to a maximum of one particle per rung. Second of all, the lower bound obtained from the Witten index for these geometries does not agree with the asymptotic value for the triangular lattice to within the error bars [36].

The results for the ladder geometries of size $4 \times L, 5 \times L, 6 \times L$ and $7 \times L$ are shown in figure 2. A fit to the data suggests that the total number of ground states on the triangular lattice of size $M \times N$ grows as

$$N_{\mathrm{gs}} \sim 1.15^{MN}. \tag{2.1}$$

This result is in agreement with the upper and lower bounds given by $(\sqrt{\phi})^{MN} \sim 1.27^{MN}$ and 1.14^{MN}, respectively.

We now turn to the range of fillings for which zero energy states exist. As explained in section 1.3, Jonsson obtained a minimal range of fillings for which zero energy states exist. We now present a maximum on this range.

Lemma 1. *The cohomology of the $M \times N$ triangular lattice is trivial for all fillings $\nu > 1/4$ and $\nu < 1/8$.*

Proof. We divide the $M \times N$ triangular lattice into two sublattices, each consisting of a set of disconnected chains. More precisely, sublattice S_1 consists of all sites with coordinates $(m, 2n)$ and sublattice S_2 consists of all sites with coordinates $(m, 2n+1)$, with $m \in \{0, \ldots, M-1\}$

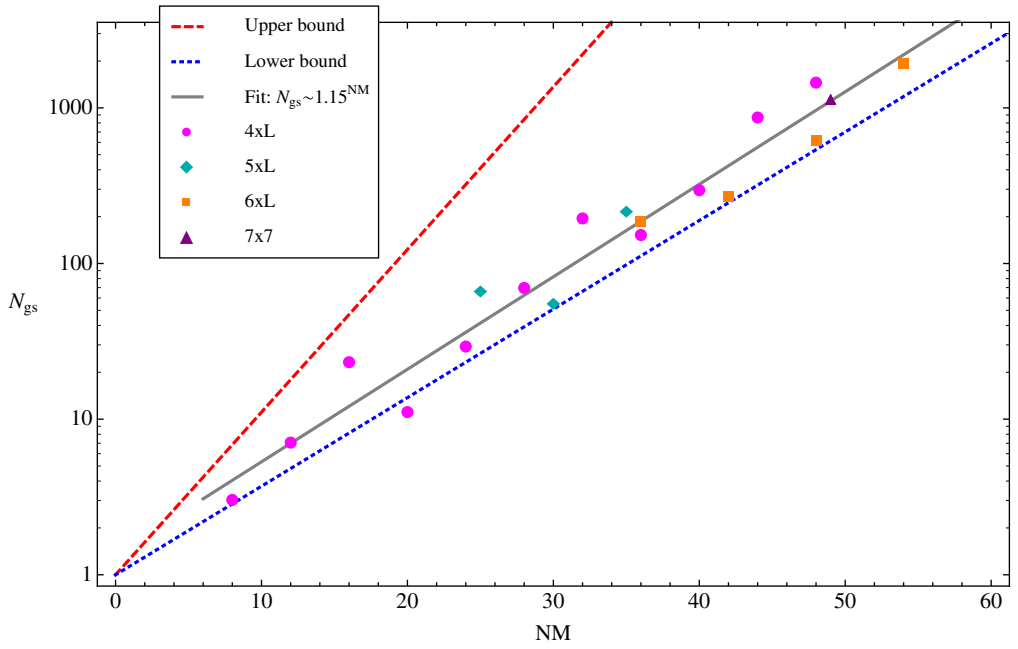

Figure 2. We plot the total number of ground states for ladder geometries of size $4 \times L$ (circles), $5 \times L$ (diamonds), $6 \times L$ (squares) and $7 \times L$ (triangles) on a logarithmic scale as a function of the total number of sites. The drawn, gray line is a fit to the data. The dotted, blue line is the lower bound and the dashed, red line is the upper bound.

and $n \in \{0, \ldots, \lfloor N/2 \rfloor - 1\}$. We now show that the cohomology of Q_2 is trivial for all fillings outside the range between $1/8$ and $1/4$.

Let us first consider the case that none of the S_1 sites are occupied. It follows that the S_2 sublattice is a collection of periodic chains. For these chains the cohomology is non-trivial at $1/3$ filling only. This results in an overall filling of 1 particle per 6 sites. It follows that non-trivial elements of $\mathcal{H}_Q$ at other fillings must have particles on the S_1 sublattice.

The highest possible overall filling is found to be $1/4$. On the one hand, maximizing the density on S_1, which is $1/2$ filled, results in an overall filling of $1/4$, since all sites on the S_2 sublattice must be empty due to nearest-neighbor exclusion. On the other hand, an effective chain of length 2 on the S_2 sublattice has a ground state with 1 particle, that is, at 1/2 filling. However, an effective open chain on the S_2 sublattice always has a blocked site at each end, leading to an effective filling of $1/4$. One readily checks that maximizing the overall filling by occupying the S_1 sublattice such that the S_2 sublattice is effectively a collection of short chains also leads to a maximal filling of $1/4$.

The minimal filling for which $\mathcal{H}_{Q_2}$ is non-trivial is obtained by blocking all S_2 sites by occupying a minimal number of sites in S_1. One quickly shows that this leads to an overall filling of $1/8$.

We conclude that $\mathcal{H}_{Q_2}$ is non-trivial for all fillings between $1/8$ and $1/4$. Using the fact $\mathcal{H}_Q \subseteq \mathcal{H}_{Q_1}(\mathcal{H}_{Q_2}) \subseteq \mathcal{H}_{Q_2}$, we establish this as the maximal range in which zero energy states can occur.

□

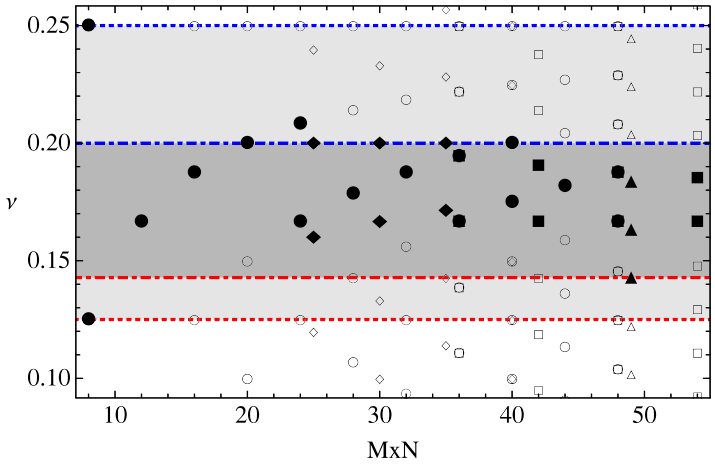

Figure 3. We plot the fillings for which zero energy states exist as a function of the total number of sites for ladder geometries of size $4 \times L$ (circles), $5 \times L$ (diamonds), $6 \times L$ (squares) and $7 \times L$ (triangles). Open symbols indicate the possible fillings for a given system size. Filled symbols indicate the fillings for which zero energy states exist. The red and blue lines are lower and upper bounds on the fillings, respectively. The dotted lines indicate the range $1/8 < \nu < 1/4$, outside this range no zero energy states exist. The dash-dotted lines indicate the range $1/7 < \nu < 1/5$, inside this range zero energy states exist for the full triangular lattice.

Numerically, we observe zero energy states for fillings $\nu \in [1/7, 1/5] \cap \mathbb{Q}$ (see figure 3). We note that the cross-cycle at $1/7$ filling obtained by Jonsson requires systems of size $M \times N$, such that both M and N are multiples of 7. We therefore only observe $1/7$ filling for the system of size 7×7. Interestingly, zero energy states at $1/5$ filling are observed even for systems with periodicities that are not compatible with the cross-cycle at $1/5$ filling. An example is the system of size 4×10. Finally, we note that although the data seems to suggest that there are no zero energy states outside the range of fillings obtained by Jonsson, we have insufficient data to go beyond speculation. It has come to our attention that the work of Galanakis *et al* [17] may shed further light on this issue.

Finally, we implemented translational invariance to obtain the ground state degeneracy per momentum sector. We resolved for momenta along both periodicities, $\vec{u} = (0, M)$ and $\vec{v} = (N, 0)$. The eigenvalues of translations along $\vec{u}$ and $\vec{v}$ we write as $t_y = \mathrm{e}^{2\pi \imath k_y/M}$ and $t_x = \mathrm{e}^{2\pi \imath k_x/N}$, respectively. The data clearly reveals a 2D flatband dispersion, that is, we typically find zero energy states for all momenta (k_x, k_y). An example is shown in table 1. We observe this property for all system sizes, with the exception of the three-leg ladder of size $3 \times L$ with L odd. We discuss this special case in more detail in section 3.2. We conclude that the triangular lattice of general size $M \times N$ will typically exhibit a 2D flatband dispersion at least for a certain range of fillings. This feature was also observed for the square lattice [21].

3. Superfrustration for three- and four-leg ladders

In this section we focus on the ladder geometries of size $3 \times L$ and $4 \times L$. For the four-leg ladder we present a slightly sharper upper bound to the total number of ground states and we conjecture

Table 1. We show the ground state degeneracy per momentum sector for the triangular lattice of size 6×9. There are zero energy states in the sector with nine (left) and 10 (right) particles. The momentum sectors are labeled by k_x and k_y as defined in the text. It is clear that there are zero energy states in all momentum sectors for both particle number sectors, indicating a 2D flatband dispersion.

6×9

$N_{gs} = 1926, W = 1462$

$f = 9$							$f = 10$						
(k_x, k_y)	0	1	2	3	4	5	(k_x, k_y)	0	1	2	3	4	5
0	9	3	3	9	3	3	0	33	31	31	33	31	31
1	4	5	3	4	5	3	1	32	31	31	32	31	31
2	4	3	5	4	3	5	2	32	31	31	32	31	31
3	7	4	4	7	3	4	3	32	32	31	32	30	31
4	4	5	3	4	5	3	4	32	31	31	32	31	31
5	4	3	5	4	3	5	5	32	31	31	32	31	31
6	7	4	3	7	4	4	6	32	31	30	32	31	32
7	4	5	3	4	5	3	7	32	31	31	32	31	31
8	4	3	5	4	3	5	8	32	31	31	32	31	31

a sharper bound on the range of filling for which zero energy states exist. We then turn to the three-leg ladder, for which we present a variety of analytic and numerical results. Interestingly, the ground state structure of this system is very different for odd and even lengths, L. For L even we find the total number of ground states for each particle number sector analytically by solving the cohomology problem, for odd L this result is still lacking. We do, however, present a rigorous lower bound on the cohomology and conjecture that it is exact [35]. Furthermore, numerical computations for the ground state degeneracy in each momentum sector clearly show a flatband for L even for momenta in both the vertical and the horizontal direction. For L odd we do not observe a flatband.

3.1. Four-leg ladder

For the four-leg ladder we have not been able to solve the full cohomology problem. However, (for L even) we can compute the cohomology of $\mathcal{H}_{Q_2}$, where Q_2 acts only on the sites of even rungs and Q_1 acts only on sites of odd rungs, such that $Q = Q_1 + Q_2$. This gives an upper bound on the full cohomology solution, since $\mathcal{H}_Q \subseteq \mathcal{H}_{Q_1}(\mathcal{H}_{Q_2}) \subseteq \mathcal{H}_{Q_2}$.

Let us define S_1 and S_2 as the sublattices consisting of the sites of odd and even rungs, respectively. To compute $\mathcal{H}_{Q_2}$ we consider all configurations on sublattice S_1 such that the cohomology of Q_2 is non-trivial. Note that the sublattice S_2 is a collection of periodic four-site chains. Particles on S_1 block sites on these chains, effectively cutting them into smaller open chains. For a given even rung in S_2 we thus have four possibilities: (1) the adjacent S_1 rungs are empty, leading to a four-site periodic chain, or the configuration on the adjacent S_1 rungs is such that the S_2 rung is effectively, (2) a two-site open chain, (3) an isolated site, (4) entirely empty (see figure 4). In all situations, there is one non-trivial element in $\mathcal{H}_{Q_2}$, except in the third situation; when the S_2 rung is effectively an isolated site the cohomology vanishes. It thus

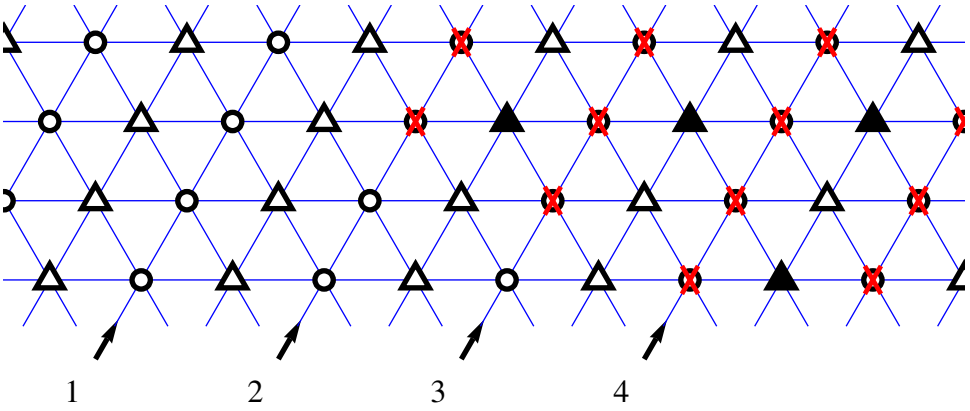

Figure 4. We show an example of a configuration on sublattice S_1 that leads to the four possible effective chains on sublattice S_2. We denote sites on sublattices S_1 and S_2 by triangles and circles, respectively. Filled triangles are occupied S_1 sites, the open triangles are empty sites. On the S_2 sublattice we indicate sites that must be empty by nearest-neighbor exclusion by the red crosses. Finally, the numbers labeling the S_2 rungs refer to the four possibilities described in the text; (1) four-site periodic chain, (2) two-site open chain, (3) an isolated site, (4) entirely empty.

quickly follows that a complete basis of representatives of $\mathcal{H}_{Q_2}$ is given by all configurations on S_1 such that there is no S_2 rung that is effectively an isolated site.

A transfer matrix generating the allowed configurations is easily constructed. We define the activity on sublattice S_i as e^{μ_i} and write $y = e^{\mu_1}$ and $x = e^{\mu_2}$. The transfer matrix for adding two rungs can then be written as

$$T_4^2(x, y) = \begin{pmatrix} x & xy & xy & xy & xy & y^2 & y^2 \\ x & 0 & xy & 0 & y & y^2 & y^2 \\ x & y & 0 & xy & 0 & y^2 & y^2 \\ x & 0 & y & 0 & xy & y^2 & y^2 \\ x & xy & 0 & y & 0 & y^2 & y^2 \\ 1 & y & y & y & y & y^2 & y^2 \\ 1 & y & y & y & y & y^2 & y^2 \end{pmatrix}. \tag{3.1}$$

We readily verify that $\mathrm{Tr}([T_4^2(-1,-1))]^n)$ correctly reproduces the Witten index results for ladders of length $2n$. The dimension of $\mathcal{H}_{Q_2}$ for a ladder of length $2n$ is given by

$$\dim(\mathcal{H}_{Q_2}(L = 2n)) = \mathrm{Tr}([T_4^2(1,1))]^n) = \sum_i \lambda_i^n = 6^n + (-2)^n + (-1)^n, \tag{3.2}$$

where λ_i are the eigenvalues of the transfer matrix, which are found to be $6, -2, -1, 0, 0, 0$. It follows that for large n, we obtain a new upper bound to the total number of zero energy states. For ladders of even length L we find it to be $(6^{1/8})^{4L} \approx 1.25^{4L}$, which is slightly sharper than the upper bound by Engström ($\sqrt{\phi}^{4L} \approx 1.27^{4L}$). The result can be extended to ladders of odd length by constructing a transfer matrix for adding two S_2 rungs and one S_1 rung. This is straightforward, but somewhat tedious. We merely state the result

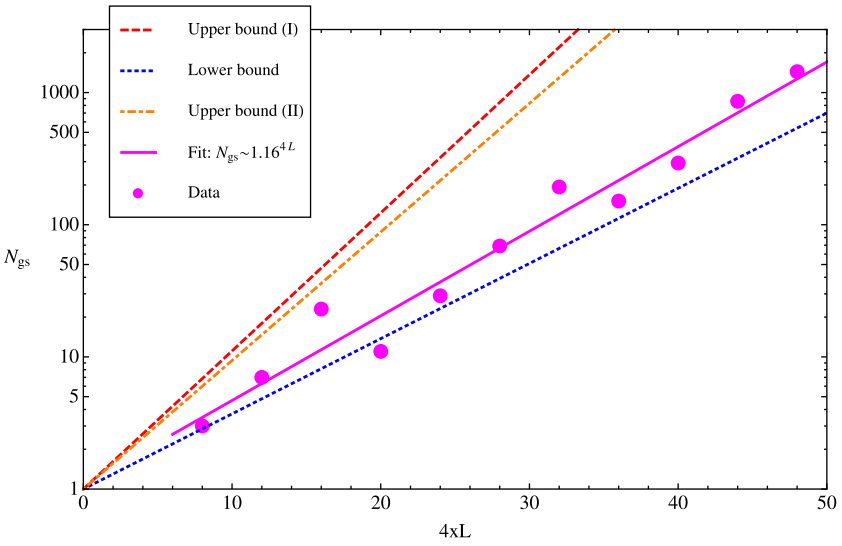

Figure 5. We plot the total number of zero energy states for the $4 \times L$ ladders on a logarithmic scale. The drawn, magenta line is a fit to the data. The dotted, blue line is the lower bound and the dashed, red line is the upper bound obtained by Engström and the dash-dotted, orange line is the upper bound from the dimension of $\mathcal{H}_{Q_2}$.

$$T_4^3(x, y) = \begin{pmatrix} 5x^2 & x^2y & x^2y & x^2y & x^2y & xy^2 & xy^2 \\ x^2 & 0 & 2xy & 2xy & 0 & xy^2 & xy^2 \\ x^2 & 0 & 0 & 2xy & 2xy & xy^2 & xy^2 \\ x^2 & 2xy & 0 & 0 & 2xy & xy^2 & xy^2 \\ x^2 & 2xy & 2xy & 0 & 0 & xy^2 & xy^2 \\ x & xy & xy & xy & xy & y^2 & y^2 \\ x & xy & xy & xy & xy & y^2 & y^2 \end{pmatrix}. \tag{3.3}$$

From this we find

$$\dim(\mathcal{H}_{Q_2}(L = 2n+1)) = \mathrm{Tr}\left(T_4^3(1, 1)[T_4^2(1, 1))]^{n-1}\right) = \frac{160}{21}6^{n-1} + \frac{5}{7}(-1)^{n-1}, \tag{3.4}$$

which leads to the same asymptotic bound on the total number of zero energy states as for the even length ladders.

In figure 5, we plot the numerically computed total number of zero energy states together with the new upper bound and the two known bounds. We see that the numerical results are consistent with these bounds. A fit to the numerical data suggests that the total number of ground states goes as $\sim 1.16^{4L}$. It is clear that the new upper bound still leaves much room for improvement.

The cohomology solution of Q_2 contains more information: it gives an upper bound on the number of zero energy states at each particle number. One easily checks that the non-trivial elements in $\mathcal{H}_{Q_2}$ have at least one and at most two particles per two rungs. This proves that there are no zero energy states for all fillings $\nu > 1/4$ and $\nu < 1/8$. In other words, we find a strict bound on the range of filling for which zero energy states can exist: $1/8 \leqslant \nu_{gs} \leqslant 1/4$. However,

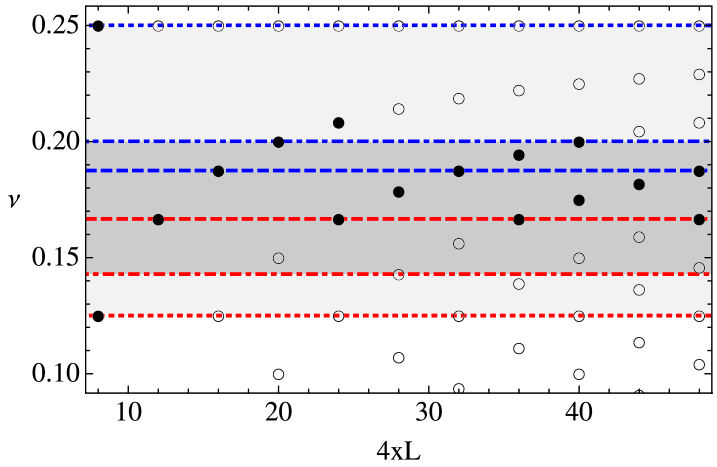

Figure 6. We plot the fillings for which zero energy states exist as a function of the total number of sites for the four-leg ladder. Open circles indicate the possible fillings for a given system size. Filled circles indicate the fillings for which zero energy states exist. The red and blue lines are lower and upper bounds on the fillings, respectively. The dotted lines indicate the range $1/8 < \nu < 1/4$, outside this range no zero energy states exist. The dash-dotted lines indicate the range $1/7 < \nu < 1/5$, inside this range zero energy states exist for the full triangular lattice. The dashed lines indicate the range $1/6 < \nu < 3/16$, inside this range zero energy states exist for the four-leg ladder.

the fact that $\dim(\mathcal{H}_{Q_2}) \gg N_{\mathrm{gs}}$ suggests that the actual range will be significantly smaller. In figure 6, we show the numerical results for the range of fillings for which zero energy states exist. The results clearly obey the strict bound. Apart from the strict bound we have also indicated the minimal range, $1/7 \leqslant \nu \leqslant 1/5$, for which zero energy states exist as shown by Jonsson. This result, however, is valid provided that the triangular lattice is wrapped on a large enough torus. For the 4 leg ladder it is easily seen that the periodicity $\vec{v} = (0, 4)$ does not accommodate the cross-cycles with $1/5$ filling or $1/7$ filling. We do find cross-cycles with $1/6$ filling and with $3/16$ filling (see figure 7). By combining their unit cells, we can construct cross-cycles for all fillings in the range $1/6 \leqslant \nu \leqslant 3/16$ provided the length of the system is long enough. This thus constitutes a strict minimum on the range in which zero energy states exist. The numerical data is in good agreement with this bound and may even suggest that for large enough L there are no zero energy states outside this range. Based on the data we are confident to conjecture that there are no zero energy states for fillings $\nu < 1/6$. For the maximal filling, however, the data is not conclusive and it might still be higher than $3/16$.

3.2. Three-leg ladder

We now consider the three-leg ladder. We start with the results that we obtain analytically: the Witten index, the solution of the cohomology of Q for L even and various bounds on the number of zero energy states and their filling for L odd.

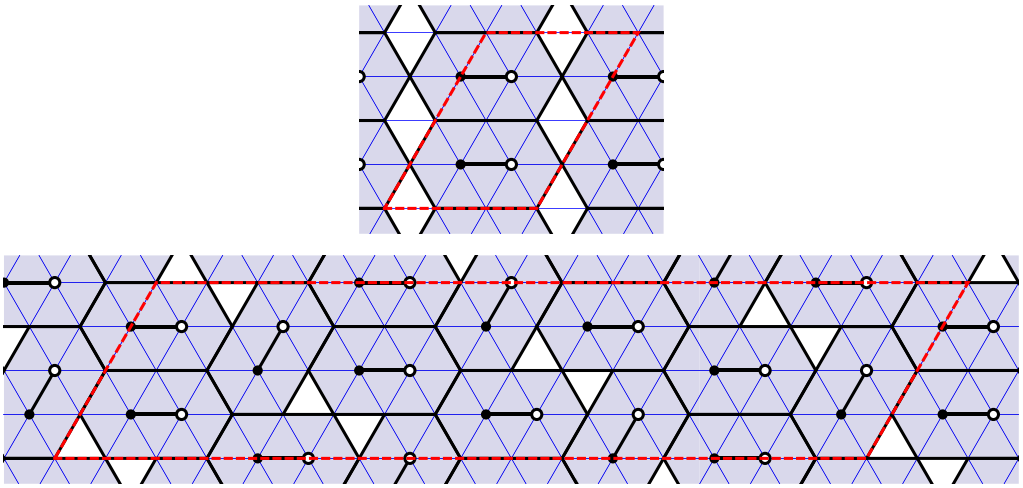

Figure 7. We show examples of cross-cycles with 1/6 (top) and 3/16 (bottom) filling (see section 1.3). We use the notation introduced in [29]; the black sites form the set $\{a_i\}$ and the white sites form the set $\{b_i\}$. Both sets form a maximal independent set. The dashed red line serves as a guide to the eye, to see that the periodicities of the cross-cycles are compatible with the four-leg ladder. The figure also shows that by concatenating the two patterns we obtain cross-cycles for all rational fillings between 1/6 and 3/16 filling provided the length of the ladder is sufficiently long.

A closed expression for the Witten index of the three-leg ladder of general length L is readily obtained from the transfer matrix that adds a single rung. The transfer matrix reads

$$T_3(z) = \begin{pmatrix} 1 & z & z & z \\ 1 & 0 & 0 & z \\ 1 & z & 0 & 0 \\ 1 & 0 & z & 0 \end{pmatrix}, \tag{3.5}$$

where we defined the activity $z = e^{\mu}$. The Witten index follows from setting the activity to -1:

$$\begin{aligned} W(L) &= \mathrm{Tr}(T_3^L(-1)) \\ &= \sum_i \lambda_i^L \\ &= 2^{L/2}\left(\mathrm{e}^{-\mathrm{i}\pi L/2} + \mathrm{e}^{\mathrm{i}\pi L/2}\right) + \mathrm{e}^{-\mathrm{i}\pi L/3} + \mathrm{e}^{\mathrm{i}\pi L/3} \\ &= 2^{L/2+1}\cos(\pi L/2) + 2\cos(\pi L/3) \\ &= \begin{cases} (-1)^{L/2}2^{L/2+1} + \delta_L, & \text{for} \quad L \text{ even}, \\ -\delta_L, & \text{for} \quad L \text{ odd}, \end{cases} \end{aligned} \tag{3.6}$$

where $\delta_L = 2$ if L is divisible by 3 and $\delta_L = -1$ otherwise (interestingly, this is the same δ_L that Jonsson introduced to write the Witten index for the square lattice [27]). Note the stark contrast between ladders of even and odd length. For the former the absolute value of the Witten index grows exponentially with system size, while for the latter the lower bound on the number of ground states is at most two.

We now consider the cohomology problem for L even. We define S_2 as the subset of all sites on the even rungs and S_1 as the rest. The cohomology of $\mathcal{H}_{Q_2}$, where Q_2 acts only on the S_2 sites is found from considering all possible configuration on S_1. For S_1 empty, S_2 consist of $L/2$ periodic chains of length 3. Each chain has two ground states with one particle. So we find that there are $2^{L/2}$ non-trivial elements in $\mathcal{H}_{Q_2}$ with $f_1 = 0$ and $f_2 = L/2$. Now if we occupy a site on S_1 it blocks two sites of the S_2 chains on the two neighboring rungs. These rungs are thus effectively isolated sites. The cohomology is then trivial unless these isolated sites are also blocked. Note that we can have at most one particle per rung. It follows that the cohomology is trivial for all $f_1 > 0$, except if $f_1 = L/2$. Upon inspection one can show that the number of ways to block all S_2 sites is

$$2^{L/2} + \delta_L(-1)^{L/2}. \tag{3.7}$$

Consequently, (3.7) gives the number of non-trivial elements in $\mathcal{H}_{Q_2}$ with $f_1 = L/2$ and $f_2 = 0$. This solves $\mathcal{H}_{Q_2}$. It is easy to show that $\mathcal{H}_{Q_1}(\mathcal{H}_{Q_2})$ has the same non-trivial elements by checking that within $\mathcal{H}_{Q_2}$ all elements are in the kernel of Q_1 and therefore not in the image of Q_1. Finally, since all elements have $f = L/2$, we immediately find $\mathcal{H}_Q = \mathcal{H}_{Q_1}(\mathcal{H}_{Q_2})$. So the number of zero energy states is

$$N_{\text{gs}}(L) = 2^{L/2+1} + \delta_L(-1)^{L/2}, \quad \text{for} \quad L \text{ even}. \tag{3.8}$$

All ground states have $L/2 = MN/6$ particles, where $MN = 3L$ is the total number of sites. This corresponds to $1/6$ filling. We find perfect agreement with these results and the numerical results for ladders of even length up to $L = 16$.

For ladders of odd length L we also study the cohomology problem. We make the same subdivision in lattices S_1 and S_2, but now S_1 consists of $(L-3)/2$ disconnected rungs and one pair of adjacent rungs. Following the same reasoning as for L even, we now find that $\mathcal{H}_{Q_2}$ consists of $2^{(L-1)/2}$ non-trivial elements with $f_1 = 0$ and $f_2 = (L-1)/2$ and $2^{(L-1)/2} + \delta_L(-1)^{(L-1)/2}$ non-trivial elements with $f_1 = (L+1)/2$ and $f_2 = 0$. Again one readily checks that $\mathcal{H}_{Q_1}(\mathcal{H}_{Q_2})$ has the same non-trivial elements. However, to obtain $\mathcal{H}_Q$ from $\mathcal{H}_{Q_1}(\mathcal{H}_{Q_2})$ is now a non-trivial step and turns out to be very challenging. We will comment on this below. We first mention a few results that we obtain directly from $\mathcal{H}_{Q_1}(\mathcal{H}_{Q_2})$. Since $\mathcal{H}_{Q_1}(\mathcal{H}_{Q_2})$ contains the cohomology of Q, it gives an upper bound on the total number of zero energy states:

$$N_{\text{gs}}(L) \leqslant \dim(\mathcal{H}_{Q_1}(\mathcal{H}_{Q_2})) = 2^{(L+1)/2} + \delta_L(-1)^{(L-1)/2}, \quad \text{for} \quad L \text{ odd}. \tag{3.9}$$

Furthermore, we find that the cohomology of Q is non-trivial only in the sectors with $(L \pm 1)/2$ particles. For large L this converges to $1/6$ filling.

In figure 8, we plot the numerical results for total number of zero energy states for L odd (see also appendix B.1). We also plot the upper bound given by the dimension of $\mathcal{H}_{Q_1}(\mathcal{H}_{Q_2})$ and the lower bound given by the Witten index. There is a clear substructure with period 3, both in the numerical data as well as in the analytic results. We thus extract the asymptotic behavior of the number of ground states by fitting to the running average of the data over three consecutive ladder lengths. We find $N_{\text{gs}} \sim 1.08^{NM}$. Note that, in contrast, for the three-leg ladder with an even number of rungs we found $N_{\text{gs}} \sim 1.12^{NM}$. This result clearly indicates that the last step in the cohomology computation, i.e. finding $\mathcal{H}_Q$ from $\mathcal{H}_{Q_1}(\mathcal{H}_{Q_2})$ is a non-trivial step. Finally, we mention that all zero energy states are found in the sectors with $(L \pm 1)/2$ particles in agreement with the result for $\mathcal{H}_{Q_1}(\mathcal{H}_{Q_2})$. We also observe that the number of zero energy states with $(L+1)/2$ particles equals the number of zero energy states with $(L-1)/2$ particles up to $\pm\delta_L$ in agreement with the Witten index.

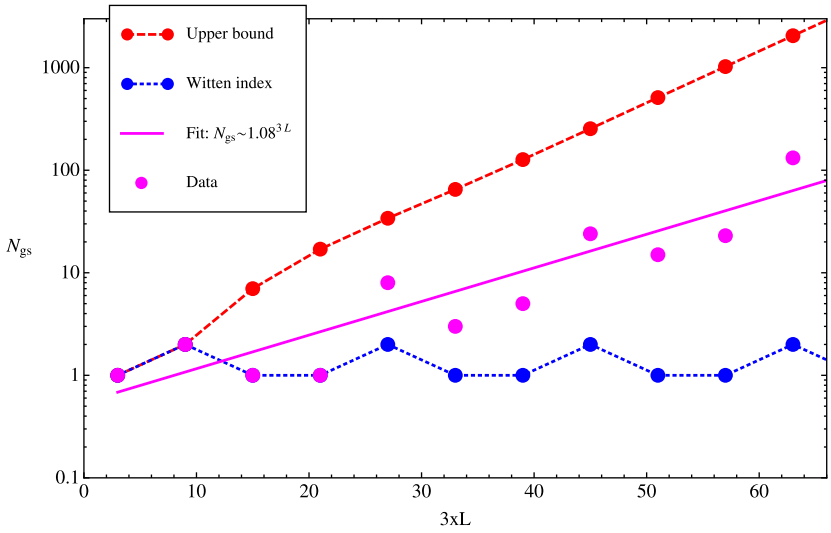

Figure 8. We plot the total number of zero energy states for the $3 \times L$ ladders with odd L on a logarithmic scale. The drawn, magenta line is a fit to the running average of the data over three consecutive ladder lengths. The dotted, blue line is a lower bound given by the absolute value of the Witten index and the dashed, red line is an upper bound on the number of zero energy states given by the dimension of $\mathcal{H}_{Q_1}(\mathcal{H}_{Q_2})$.

The numerical results for the number of zero energy states, not only resolve for particle number, but also for momentum along the legs and the rungs of the ladder. For the three-leg ladder this data reveals again a very different structure for ladders with even length and ladders with odd length. For the ladders with L even the number of zero energy states is distributed evenly over all momentum sectors. This implies that there is a completely flat dispersion relation in all directions. This flatband property was also observed for the supersymmetric model on the square lattice [21]. For the square lattice this could be understood from a mapping of the cohomology elements onto tilings [21, 25, 27]. The unit cell of a tiling directly translates into the eigenvalues under translations of the corresponding ground state. For the three-leg ladder we also find a correspondence between representatives of the cohomology and tilings. An example is shown in figure 10. There are two tiles and each tile can be neighbored by both tiles (this corresponds to the fact that the ground state degeneracy goes as $2^{L/2}$). It is easy to see that there are many possible tilings with a unit cell equal to the size of the system. Each such tiling thus corresponds to $3L$ ground states, one in each momentum sector. This explains the observed flatband. Tilings with a smaller unit cell correspond to ground states that occur only in certain momentum sectors. We have checked that for finite systems a careful analysis of all tilings and their properties under translations indeed reproduces the distribution of ground states over momentum sectors as found in the numerics (for an explicit example see appendix B.2). We note that just as for the square lattice the correspondence between cohomology elements and tilings is not exactly one-to-one. In fact, we find

$$N_{\mathrm{gs}}(L) = N_{\mathrm{tilings}}(L) + \delta_L(-1)^{L/2}, \tag{3.10}$$

which is remarkably similar to the result obtained for the square lattice.

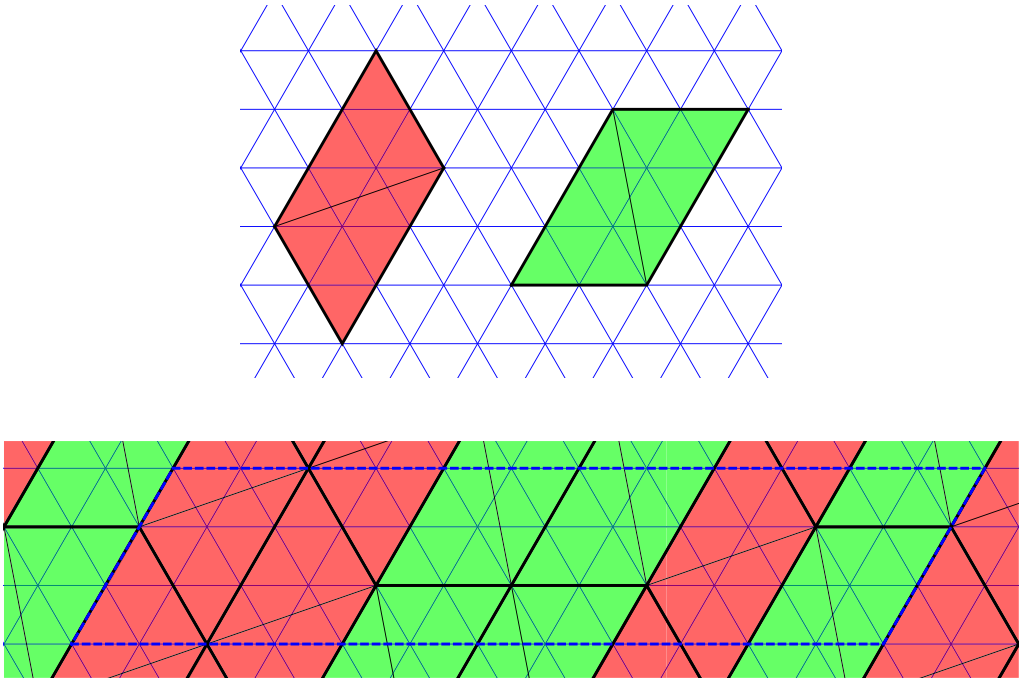

Figure 9. Tilings on the three-leg ladder. Above we show the two allowed tiles in red and green. Note that it is the same tile with two possible orientations, the third orientation is not compatible with the boundary conditions. Below we show an example of a tiling with periodicities $\vec{u} = (0, 3)$ and $\vec{v} = (12, 0)$.

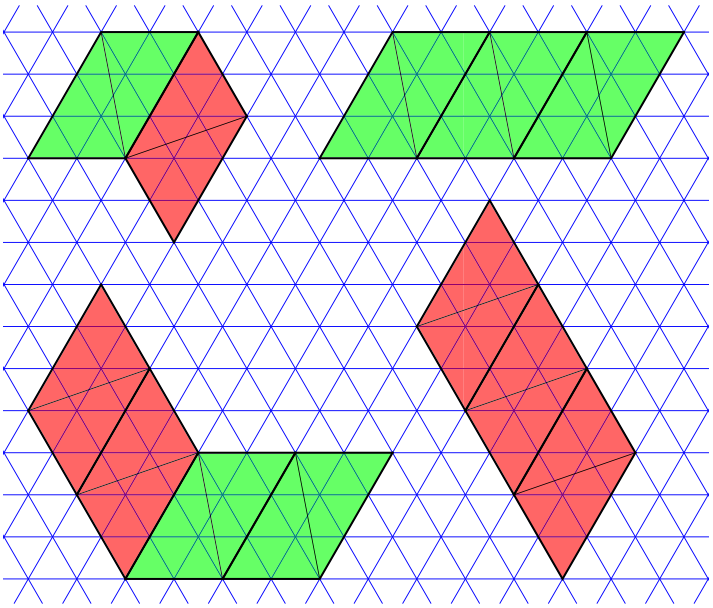

Figure 10. We show the four types of tiles that are used to construct cohomology elements for the three-leg ladder of odd length, L. Note that the tiles are composed of the two tiles introduced for the three-leg ladder of even length (see figure 9).

For the three-leg ladder with L odd we observe the following. When L is a multiple of 3 there are zero energy states in the sectors with $p_x = 2\pi - p_y = 2\pi k/3$, with $k = 0, 1, 2$. When L is not a multiple of 3 all zero energy states have $p_x = p_y = 0$. The substructure with period 3 in the system size is again apparent.

The results presented in this section clearly indicate that the cohomology problem for $3 \times L$ with L odd is highly non-trivial. Nevertheless, we have been able to make substantial progress beyond the results mention above. We believe a complete solution is possible and hope to present it in forthcoming work [35]. At this point we present a rigorous lower bound on the number of ground states.

Lemma 2. *The number of zero energy states, $N_{\rm gs}$, for the $3 \times L$ triangular lattice with L odd obeys:*

$$N_{\rm gs} \geqslant \text{const} \times [(\phi)^{1/6}]^{3L} \sim \text{const} \times 1.08^{3L}, \tag{3.11}$$

with $\phi = \frac{1}{2}(1+\sqrt{5})$, the golden ratio.

This lower bound agrees with the exponential growth observed in the numerical data. We limit ourselves to a short sketch of the proof of this lower bound and defer the details to [35].

The key ingredient is to compute $\mathcal{H}_{Q_1}(\mathcal{H}_{Q_2})$ for a different choice of the sublattices S_1 and S_2. Instead of the choice discussed above, we now take S_1 to be one rung and S_2 the rest of the system. S_2 is thus an open three-leg ladder of even length. The cohomology of Q_2 is still easily obtained for this choice of sublattice, however, we pay extra care to choose the basis in such a way that the action of Q_1 is relatively simple. As before we find that the number of non-trivial elements in $\mathcal{H}_{Q_2}$ is $2^{(L+1)/2} + \delta_L(-1)^{(L-1)/2}$, however, we now find that $2^{(L-1)/2}$ of these elements have $f_1 = 0$ and $f_2 = (L-1)/2$ and $2^{(L-1)/2} + \delta_L(-1)^{(L-1)/2}$ of these elements have $f_1 = 1$ and $f_2 = (L-1)/2$. As a consequence, the next step in the cohomology computation, that is, finding $\mathcal{H}_{Q_1}(\mathcal{H}_{Q_2})$, is now non-trivial. The upshot is that for this construction we immediately have $\mathcal{H}_Q = \mathcal{H}_{Q_1}(\mathcal{H}_{Q_2})$. It is possible to express the action of Q_1 on the non-trivial elements of $\mathcal{H}_{Q_2}$ in a general form, that is for general length L. From these expressions, we can identify certain linear combinations of the basis elements of $\mathcal{H}_{Q_2}$ that are annihilated by Q_1 up to terms that are in the image of Q_1. These elements are thus in $\mathcal{H}_{Q_1}(\mathcal{H}_{Q_2})$. For $L \equiv 0 \bmod 3$ we find that these elements can be written as sequences of tiles on S_2. More precisely, we can identify an element of $\mathcal{H}_{Q_1}(\mathcal{H}_{Q_2})$ with each tiling of S_2 up to cyclic shifts. The rigorous lower bound then follows from counting the number of these tilings (note that the reduction due to cyclic shifts is at the worst a factor of $2/(L-1)$, which does not affect the exponential behavior). The tilings consist of four types of tiles depicted in figure 10.

The counting of the tilings is easily done. We define $t(l)$ as the number of tilings at $L = 2l + 1$. The counting of $t(l)$ leads to a recursion

$$t(l) = t(l-2) + t(l-4) + 2t(l-3). \tag{3.12}$$

The characteristic equation has a factor $(x^2 - x - 1)$ and the largest eigenvalue is the golden ratio $\phi = (1+\sqrt{5})/2$. The number of ground states grows as $(\phi^{1/6})^{3L} \sim 1.08^{3L}$ in agreement with the numerical results. The resulting value for the ground state entropy per site is

$$S_{\rm gs}/(3L) \geqslant \log(\phi)/6 \sim 0.080. \tag{3.13}$$

We conclude that other than for L even, the system hesitates between two values for the number of particles in the ground state, $L/6 \pm 1/2$. This gives a cancelation that reduces the number of

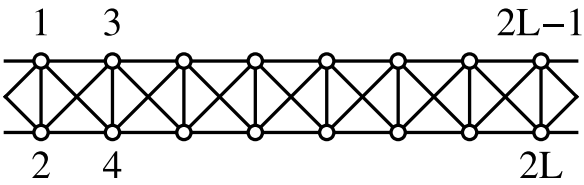

Figure 11. The two-leg ladder of length L, with sites labeled $1, \ldots, 2L$.

ground states we see for L even, $2^{1/6}$, to the smaller number given above. Other than is suggested by the Witten index, the growth is still exponential in L. This is the second example, after the analysis for the square lattice [25], where a non-trivial ground state degeneracy is derived from a tiling argument. At this instance the analysis is less complete though, since the full solution of the cohomology problem is still open.

4. Complete solution for the two-leg ladder

In this section, we discuss the simplest ladder obtained from the triangular lattice by imposing the periodicities $\vec{u} = (0, 2)$ and $\vec{v} = (L, 0)$. The resulting ladder geometry is depicted in figure 11. This lattice is special because it is invariant under the exchange of the two sites on a rung. A state on the lattice will have either even or odd parity under this transformation. Consequently, this local $\mathbb{Z}_2$ symmetry distinguishes an exponential number of sectors. This observation will allow us to understand the exponential ground state degeneracy. Furthermore, we find a mapping from the ladder to the chain such that the entire spectrum can be understood. Remarkably, in certain sectors the spectrum turns out to be gapped, in others it is gapless and in yet other sectors we find phase separation. The continuum limit of each of the gapless sectors is shown to be described by a superconformal field theory with central charge $c = 1$.

4.1. Mapping the ladder to an infinite number of chains

In this section, we present a mapping that maps the supersymmetric model on the ladder onto the supersymmetric model of a collection of chains. As a first step we write the three possible states on a rung i, that connects the sites $2i - 1$ and $2i$, as follows: the empty rung, which we denote by $|0\rangle_i$ and two states with one particle on the rung:

$$|\pm\rangle_i = \frac{1}{\sqrt{2}} \left(c^\dagger_{2i-1} \pm c^\dagger_{2i} \right) |0\rangle_i . \tag{4.1}$$

The next thing to note is that the state $|-\rangle_i$ is localized and carries zero energy. The localization is due to the fact that there is negative interference for the particle to hop off the rung. The state has zero energy because the hopping within the rung precisely cancels the potential energy of the state. The effect of these localized zero energy states on the rungs is that they effectively cut the ladder into smaller ladders with open boundary conditions.

Another way to understand this breaking up of the Hilbert space is via the parity operator, T_i, that interchanges the sites $2i - 1$ and $2i$. One easily checks that the Hamiltonian commutes with this operator. It follows that the parity on each rung is a good quantum number that is conserved under the action of the Hamiltonian. Clearly, the state $|-\rangle_i$ has odd parity under this

transformation, whereas the states $|0\rangle_i$ and $|+\rangle_i$ have even parity. The Hilbert space breaks up into disconnected sectors characterized by the parity of each rung.

One thing that is important to note is that the rungs neighboring a rung with odd parity must be empty due to the nearest-neighbor exclusion and must thus have even parity.

Suppose that the parity of two rungs that are $2+L_+$ rungs apart is odd and that all rungs in between these two rungs have even parity. It follows that there are L_+ consecutive rungs that can be in either of the two even parity states. We will now show that the Hamiltonian acting on these L_+ consecutive rungs with even parity maps to the supersymmetric Hamiltonian on the chain of length L_+ up to an overall factor of 2. In this mapping the empty rung will map to the empty site on the chain and the state $|+\rangle_i$ will map to occupied site on the chain. It is easy to see that the Hilbert spaces are indeed identical. On the chain there are two states per site, on the ladder there are two states per rung, furthermore, the nearest-neighbor exclusion ensures on the ladder that two neighboring rungs cannot both be in the $|+\rangle$ state and on the chain that two neighboring sites cannot both be occupied.

Let us introduce the creation operator $\tilde{c}_i^\dagger \equiv (c_{2i-1}^\dagger + c_{2i}^\dagger)/\sqrt{2}$, which creates the $|+\rangle_i$ from the empty rung. Furthermore, we introduce the number operator $\tilde{n}_i = n_{2i-1} + n_{2i}$ and the projection operator $\tilde{P}_{\langle j\rangle} = (1-\tilde{n}_{(j-1)})(1-\tilde{n}_{(j+1)})$. Note that the latter is indeed a projection operator, because due to the nearest-neighbor exclusion $\tilde{n}_i$ only takes the values 0 or 1. When we label the L_+ even parity rungs 1 through L_+, the Hamiltonian on that part of the system reads

$$H_+ = H_{\text{kin}} + H_{\text{pot}} = \sum_{i=0}^{2L_+} \sum_{j\in\langle i\rangle} P_{\langle i\rangle} c_i^\dagger c_j P_{\langle i\rangle} + \sum_{i=0}^{2L_+} P_{\langle i\rangle}. \tag{4.2}$$

Expanding these terms and carefully doing the algebra, we can rewrite this Hamiltonian in terms of the operators we just introduced which are defined on a chain of L_+ sites (we have deferred the details to appendix A). What we find is

$$H_+ = \sum_{j=1}^{L_+} \sum_{i=j\pm1} 2\tilde{P}_{\langle j\rangle} \tilde{c}_j^\dagger \tilde{c}_i \tilde{P}_{\langle i\rangle} + \sum_{j=1}^{L_+} 2\tilde{P}_{\langle j\rangle} = 2H_{\text{chain}}, \tag{4.3}$$

which is precisely twice the Hamiltonian on a chain of L_+ sites with an additional empty site on each end of the chain. This is equivalent to saying that the chain has open boundary conditions. Finally, we note that the Hamiltonian in the sector where all rungs of the ladder have even parity maps to the Hamiltonian on the chain with periodic boundary conditions, again up to a factor of 2. It follows that in the sector with odd parity on the rungs $\{l_1, \ldots, l_s\}$ and even parity on all other rungs, the Hamiltonian on the 2 leg ladder takes the form

$$H = 2\sum_{m=1}^{s} \left[\sum_{j=l_m+1}^{l_{m+1}-1} \left(\sum_{i=j\pm1} \tilde{P}_{\langle j\rangle} \tilde{c}_j^\dagger \tilde{c}_i \tilde{P}_{\langle i\rangle} + \tilde{P}_{\langle j\rangle} \right) \right], \tag{4.4}$$

where we defined $l_{s+1} \equiv l_1$.

This mapping is very powerful because we have very good understanding of the supersymmetric model on the chain [15, 20]. In the next sections, we will first see how we can use it to get a closed expression for the number of zero energy states and then how it allows us to fully understand the low lying spectrum.

4.2. Ground state partition sum

In the previous paragraph, we have seen that the state with odd parity on the rung is a dark state: it is localized and decoupled from the rest of the system. In addition it carries zero energy. The effect of these zero energy states is that they effectively cut the ladder into smaller ladders. These smaller ladders can be mapped to the chain, for which we know the number of zero energy states. Remember that the chain of length 1 mod 3 has no zero energy states. It follows that in a zero energy state on the ladder the number of rungs separating two odd parity rungs cannot be $3l$ rungs apart. This is because the even parity rungs will map to an open chain of length $3l-2$ for which there is no zero energy state.

Carefully counting the number of zero energy states this way, one obtains the ground state partition sum as a function of the fugacity z:

$$\begin{aligned} Z_L(z) &\equiv \mathrm{Tr}_{\mathrm{GS}} z^F \\ &= z(Z_{L-2}(z) + 2Z_{L-3}(z)) - \Delta_L, \end{aligned} \tag{4.5}$$

with

$$\Delta_L = \begin{cases} 0, & \text{for} \quad L = 3l \quad \text{and} \quad L = 3l-1 \\ z^{l+1} + z^l, & \text{for} \quad L = 3l+1 \end{cases}. \tag{4.6}$$

Since the number of sites, NM, of the ladder is $2L$, it follows immediately from the recursion relation that there will be zero energy states for $f/(NM) \in [1/6, 1/4]$.

To obtain the number of zero energy ground states we solve the recursion relation for $Z_L(z)$ and set $z = 1$. Using $Z_2 = 3z$, $Z_3 = 5z$ and $Z_4 = 2z^2 + z$, we find

$$Z_{L=3l+a}(z=1) = (-1)^L \lambda_1^{L/2} + (-1)^L (\lambda_2)^{L/2} + \lambda_3^{L/2} - (-1)^a, \tag{4.7}$$

with $a = -1, 0, 1$ and $\lambda_{1,2}$ and λ_3 the complex and real solutions to $-4 + \lambda - 2\lambda^2 + \lambda^3 = 0$, respectively. Note that $\lambda_2^* = \lambda_1$. For large L, we have

$$Z_L(z=1) \approx \lambda_3^{L/2} \approx 1.5214^L. \tag{4.8}$$

It follows that the ground state entropy per site is

$$S_{\mathrm{GS}} = \frac{1}{2L} \ln Z_L \approx \frac{\ln 1.5214}{2} = 0.2098\ldots \tag{4.9}$$

Equivalently, the Witten index is obtained by setting $z = -1$. We find

$$W_L = \left(\frac{-1 + \mathrm{i}\sqrt{7}}{2}\right)^L + \left(\frac{-1 - \mathrm{i}\sqrt{7}}{2}\right)^L. \tag{4.10}$$

For large L the Witten index grows as $\sim 1.14^L$.

4.3. Spectrum

4.3.1. Gapped at 1/4 filling. For L even there are two zero energy states with $L/2$ particles. The two ground states are product states of resonating single particle states ($|-\rangle$) on every other rung. One of the states has particles resonating on all odd rungs, the other on all even rungs. For f even (odd) translation by two rungs maps each ground state to $-(+)$ itself, so the eigenvalue of the translation operator obeys: $t^2 = -1$ for f even and $t^2 = 1$ for f odd. It follows that the

translationally invariant ground states have momenta:

$$p_1 = \pi/2 \text{ and } p_2 = 3\pi/2, \text{ for } f \text{ even}$$
$$p_1 = 0 \text{ and } p_2 = \pi, \text{ for } f \text{ even}.$$

Note that quarter filling is the highest possible density for this system due to the nearest-neighbor exclusion.

For L odd the maximal number of particles in the system is $(L-1)/2$. We find that there are $2L$ zero energy states with $f = (L-1)/2$. Pictorially, we can write these states as

$$|A\rangle = |0\rangle \prod_{k=1}^{f} |0-\rangle \quad \text{and} \quad |B\rangle = (|+0\rangle - |0+\rangle)/\sqrt{2} \prod_{k=1}^{f-1} |0-\rangle, \tag{4.11}$$

where 0 denotes an empty rung and $\pm$ denote the single particle states with even and odd parity, respectively. Clearly, there are L states of each type. These L states are related by translations by one rung. It follows that the translationally invariant ground states have momenta $p_k = 2\pi k/L$ with $k = 0, \ldots, L-1$ and there are two in each momentum sector. The two types of states occur in different parity sectors: the states of type A occur in the sector with f rungs with odd parity and the states of type B occur in the sector with $f-1$ rungs with odd parity. Note that in the latter sector, there can be four consecutive rungs with even parity, which can be mapped to a two-site open chain. Indeed, the ground state on a two-site open chain is $(|\bullet\circ\rangle - |\circ\bullet\rangle)/\sqrt{2}$.

At quarter filling there is a gap to charge–neutral excitations. The excitations at quarter filling follow from changing one of the single particle states from $|-\rangle$ to $|+\rangle$. This costs an energy $\Delta = 2$. For L even there are L such excitations, whereas for L odd there are $L^2 - 2L$ such excitations[8]. Consequently, the spectrum is gapped to chargeless excitations, the gap is $\Delta = 2$ and the first band above the ground state is completely flat. Two $|+\rangle$-excitations obey a certain exclusion statistics, so the distribution of states over the momentum sectors is not uniform, but the band is still flat at $E = 2\Delta = 4$. Continuing this way, the highest energy state is reached at $E = L$ for L even (for L odd the highest energy state is found to have $E = L+1$).

4.3.2. Gapless at 1/6 filling. At 1/6 filling the number of ground states is exponential in the length. In the sector with even parity on all rungs there are two zero energy states with $f = j$ for $L = 3j$ corresponding to the two ground states of the periodic chain of length $L = 3j$. Similarly, there is one zero energy states with $f = j$ for $L = 3j \pm 1$ corresponding to the ground state of the periodic chain of length $L = 3j \pm 1$. In the sector with j rungs with odd parity, the zero energy states can be depicted as

$$|\mathrm{gs}\rangle = \begin{cases} |0-0\rangle \prod_{k=1}^{j-1} |0-0\rangle, & \text{for} \quad L = 3j, \\ |00-\rangle \prod_{k=1}^{j-1} |0-0\rangle, & \text{for} \quad L = 3j+1, \\ |-0\rangle \prod_{k=1}^{j-1} |0-0\rangle, & \text{for} \quad L = 3j-1. \end{cases} \tag{4.12}$$

These states are clearly product states, which implies a finite correlation length and thus a gap to charge–neutral excitations. In contrast the ground states in the sector with even parity on all rungs, correspond to the ground states on a chain, which are known to be critical. It follows

[8] Note that for L odd there is the extra possibility of leaving the $|-\rangle$ states intact, but exciting the length 2 ladder to its first excited state; however, this costs an energy $\Delta = 4$.

that the spectrum is gapless in that sector. In fact, the supersymmetric model on the chain is well understood and the low-energy spectrum is known to be described by an $\mathcal{N} = (2, 2)$ superconformal field theory with central charge, $c = 1$ [15, 20]. In [20], a complete identification between states in the spectrum of chains of finite length and fields in the continuum theory is given. This identification allows us to compute the gap scaling for the two-leg ladder in each parity sector. Interestingly, we will find that the lowest non-zero energy state is not in the sector with even parity on all rungs.

The finite-size scaling of the energy of a gapless system depends on the boundary conditions:

$$E_{\text{chain}} = b\pi E_{\text{SCFT}} v_{\text{F}}/L + \mathcal{O}(1/L^2), \tag{4.13}$$

with $b = 1$ for open and $b = 2$ for periodic boundary conditions. For the supersymmetric model on the chain the Fermi velocity was found to be $v_{\text{F}} = 9\sqrt{3}/4$ [20]. For the periodic chain the first excited states have $E_{\text{SCFT}} = 2/3$ for $L = 3j$ and $E_{\text{SCFT}} = 1/3$ for $L = 3j \pm 1$. Using the fact that $H = 2H_{\text{chain}}$, we find that the finite-size energies of these states on the ladder are

$$E_{\text{ladder}} = \pi E_{\text{SCFT}} 9\sqrt{3}/L = \begin{cases} 6\pi\sqrt{3}/L, & \text{for} \quad L = 3j \\ 3\pi\sqrt{3}/L, & \text{for} \quad L = 3j \pm 1. \end{cases} \tag{4.14}$$

For the open chain with $L = 3j$ and $L = 3j - 1$ we find that $E_{\text{SCFT}} = 1$ for the first excited state. However, for the open chain of length $L = 3j + 1$ there is no zero energy state. Instead the lowest energy state at $f = j$ has $E_{\text{SCFT}} = 1/3$ and this state has a superpartner with the same energy at $f = j + 1$. Using the above, we find that the finite-size energies of these states on the ladder are

$$E_{\text{ladder}} = \frac{\pi E_{\text{SCFT}} 9\sqrt{3}}{2L} = \begin{cases} 9\pi\sqrt{3}/(2L), & \text{for} \quad L = 3j \quad \textit{and} \quad L = 3j - 1, \\ 3\pi\sqrt{3}/(2L), & \text{for} \quad L = 3j + 1. \end{cases} \tag{4.15}$$

Comparing all the above energies, we find that the lowest non-zero energy state of a ladder of length L corresponds to a state on an open chain of length $3m + 1 = L - x$, with $x = 3, 5, 7$ for $L = 3j + 1, 3j, 3j - 1$, respectively. The scaling of the energy of the first excited state thus reads

$$E_1 = \frac{3\pi\sqrt{3}}{2(3m+1)} = \begin{cases} \dfrac{3\pi\sqrt{3}}{2(L-3)}, & \text{for} \quad L = 3j + 1, \\ \dfrac{3\pi\sqrt{3}}{2(L-5)}, & \text{for} \quad L = 3j, \\ \dfrac{3\pi\sqrt{3}}{2(L-7)}, & \text{for} \quad L = 3j - 1. \end{cases} \tag{4.16}$$

The corresponding states are found in the sectors with odd parity on the rungs $\{l\}$, $\{l, l+2\}$ and $\{l, l+2, l+4\}$, respectively, where $l \in (1, \ldots, L)$. Note that the states on the chains have $f = j - 1, j - 2, j - 3$, respectively, so that the total number of fermions is always $f = j$. There are no zero energy states in these sectors. Finally, it is clear that the first excited state is L-fold degenerate: one for each momentum sector $p_k = 2\pi k/L$.

Numerical results for ladders up to $L = 23$ confirm these observations. In particular, a finite-size scaling analysis shows that the energy of the first excited state is nicely fitted with

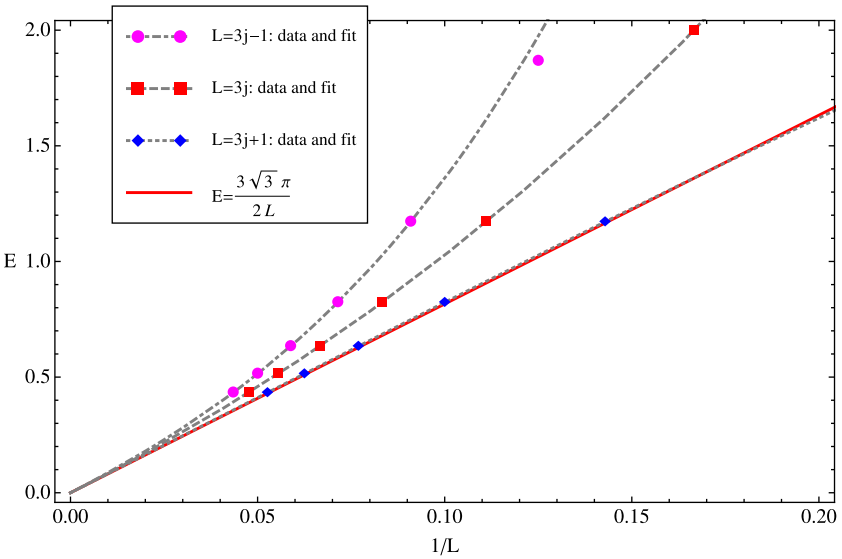

Figure 12. We plot numerical results for the energy of the first excited state of the two-leg ladders as a function of $1/L$. There is a clear substructure in the length modulo 3, which we emphasize by using different symbols and colors. The dashed/dotted lines are fits to the three data sets distinguished by their value of L mod 3 with the function $a_1/L + a_2/L^2 + a_3/L^3$. The red line is the theoretical value for the energy to order $1/L$ as derived in the text.

$a_1/L + a_2/L^2 + a_3/L^3$ (see figure 12). We extract $a_1 \approx 8.17$ for $L = 3j+1$ and $a_1 \approx 8.15$ for $L = 3j$, which is good agreement with the theoretical value $3\pi\sqrt{3}/2 \approx 8.162$. The result for $L = 3j-1$ ($a_1 \approx 8.42$) is less accurate. Indeed, from (4.16) it is clear that for this length the finite-size corrections are the strongest.

4.3.3. Phase separation at intermediate fillings. We can continue the logic of the previous section to infer the energy of the first excited state for fillings $f/(2L) \in [1/6, 1/4]$. Starting from the $1/6$ filling side, there are two obvious possibilities for the first excited state at higher densities: the density is increased either by having more particles in the part of the system where all rungs have even parity, or by going to a parity sector where for a larger part of the ladder even and odd parity rungs alternate. From the continuum theory we know that in the first case the energy scales parabolically with the fermion number:

$$E_{\mathrm{SCFT}}(\tilde{f}) = \frac{3}{2}\tilde{f}^2 - \frac{1}{2}\tilde{f}, \tag{4.17}$$

where $\tilde{f} = f_{\mathrm{chain}} - f_{\mathrm{gs}} - 1/3$. For the ladder we thus have that the energy of such states with $f = j + j'$ particles scales as

$$E(j') = \frac{9\pi\sqrt{3}}{2}\frac{1}{L-x}\left(\frac{3}{2}\tilde{f}^2 - \frac{1}{2}\tilde{f}\right) \tag{4.18}$$

$$= \frac{3\pi\sqrt{3}}{L-x}\left(\frac{1}{2} + \frac{9}{4}(j'^2 - j')\right), \tag{4.19}$$

where $x = 3, 5, 7$ for $L = 3j+1, 3j, 3j-1$, respectively.

In the second case, one can show that the first excited state with $f = j + j'$ particles corresponds to the lowest energy state of a chain of length $3m' + 1 = L - 6j' - x$ with m' fermions for j' even, and x as before. For j' odd we have $3m' + 1 = L - 6(j' - 1) - x$ with $m' + 1$ fermions. It follows that the energy of this state is

$$E(j') = \frac{3\pi\sqrt{3}}{2}\frac{1}{3m'+1} \tag{4.20}$$

$$= \frac{3\pi\sqrt{3}}{L-x}\left(\frac{1}{2} + \frac{3j'}{L-x} + \frac{18j'^2}{(L-x)^2}\right) + \mathcal{O}(j'^3), \tag{4.21}$$

for j' even and similarly for j' odd with j' replaced by $j' - 1$ everywhere. It is readily checked that for $j' > 0$, this energy is always smaller than the energy for the first case (4.18).

It follows that at some intermediate filling between $1/6$ and $1/4$, the lowest energy states show phase separation, where part of the ladder is in the $|0-0\ldots-0\rangle$ phase and the rest is in the $1/6$ filled critical phase. So starting from $1/6$ filling, both charged and charge–neutral excitations above the ground state manifold are gapless. We know, however, that at $1/4$ filling, there is a gap to charge–neutral excitations. The question is thus at what filling this gap opens up. Suppose the density is $1/4 - \epsilon$ in the thermodynamic limit. We know that the first excited state shows phase separation. The energy of the first excited state will scale as $1/l$, where l is the length of the part of the system that is in the $1/6$ filling phase. One easily checks that $l \propto \epsilon L$. It follows that for any finite ϵ the gap collapses.

Finally, we note that using parity the gapless phase separates into an exponential number of sectors[9]. In the continuum limit, each of these sectors is described by a (sum of) superconformal field theories with central charge $c = 1$.

4.4. Relation to other superfrustrated ladders

In this section, we briefly discuss two other ladder geometries that share certain properties with the two-leg ladder obtained from the triangular lattice.

The first is the octagon-square ladder depicted in figure 13, which can be obtained from the octagon-square lattice by imposing doubly periodic boundary conditions. The solution to the cohomology problem for the supersymmetric model on the octagon-square lattice is known for general boundary conditions [14]. For the octagon-square ladder with N plaquettes, the number of zero energy states is $2^N + 1$. This exponential ground state degeneracy can be understood in terms of a local symmetry, just as for the triangular ladder. Let us label the sites around a plaquette in a clockwise direction starting at the leftmost site as $i, i+1, i+2, i+3$. It follows that the sites $i+1$ and $i+3$ are connected by the link across the plaquette. It is clear that the

[9] To obtain an estimate of the number of gapless sectors in the continuum we proceed as follows. As a sufficient condition for the sector to be gapless, we require that there is at least one part of the system, say L_g consecutive rungs, with even parity, such that L_g goes to infinity as L goes to infinity. To make things concrete, let us take $L_g = L/2$. The parity of the rungs in the rest of the system then merely has to be such that a zero energy state exists. From the ground state partition function, 4.8, we easily see that the number of sectors that obey these conditions can be estimated as $\sim 1.5^{L-L_g} = 1.5^{L/2}$. This shows that there is indeed an exponential number of gapless sectors.

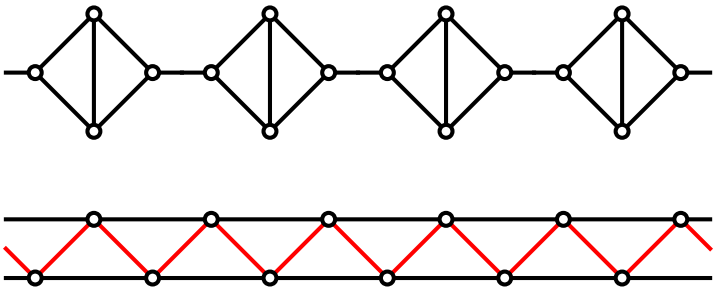

Figure 13. We show the octagon-square ladder (above) and the zig-zag ladder (below). In the octagon-square ladder the vertical links are referred to in the text as links across the plaquette. This example shows a ladder of four plaquettes. In both cases periodic boundary conditions in the horizontal direction are implied. In the zig-zag ladder, the red line serves as a guide to the eye to see that the zig-zag ladder is a chain with nearest and next-nearest-neighbor interactions.

ladder is invariant under the exchange of these two sites. Moreover, the odd parity single particle state, $|-\rangle_i \equiv (c^\dagger_{i+1} - c^\dagger_{i+3})/\sqrt{2}|\emptyset\rangle$, is again a dark state with zero energy. So having odd parity on a plaquette effectively cuts the ladder into an open ladder. Finally, there is again a mapping to the chain Hamiltonian if one restricts to the sector with even parity on the plaquettes [10]. There are three main differences. Firstly, there are zero energy states for all parity sectors. This can be seen as follows. The odd parity plaquettes cut the ladder into smaller ladders of lengths $l_j = 0 \bmod 3$ for all j. It follows that there is one zero energy state in all parity sectors, except in the sector with even parity, where we effectively have a periodic chain of length $3N$ which has two zero energy states. Note that there are 2^N parity sectors and thus $2^N + 1$ zero energy states. Secondly, all zero energy states have filling 1/4. Remember that the ground states on chains of length $l = 0 \bmod 3$ have one particle on every three sites, which corresponds to one particle per plaquette. Clearly, the plaquette with odd parity also have one particle per plaquette. Therefore, all ground states have $1/4$ filling. Thirdly, and most importantly, the spectrum is not described by a conformal field theory. This can be seen by carefully carrying out the mapping to the chain. One then finds that the effective Hamiltonian is the Hamiltonian for the staggered chain, $H = \{Q_\lambda, Q^\dagger_\lambda\}$, with $Q_\lambda = \sum_j \lambda_j c_j P_{\langle j\rangle}$, and staggering $\lambda_j = \sqrt{2}$ for $j = 0 \bmod 3$ and $\lambda_j = 1$ otherwise. This model was studied in detail in [11, 12, 22] and has a gapped spectrum, unless the boundary conditions are such that they allow for a massless kink. A massless kink exists on open chains of length $l \equiv 0 \bmod 3$ and has a $1/l^2$ dispersion. It follows that certain sectors of the octagon-square ladder are gapless, but not conformal, and others are gapped.

The second model to which our two-leg ladder bears certain similarities is the zig-zag ladder (see figure 13). This ladder is obtained from the square lattice by imposing periodicities $\vec{u} = (1, 2)$ and $\vec{v} = (L, 0)$. The similarities are not as striking as those observed for the octagon-square ladder, but we believe that they can be quite useful in trying to get a better understanding of the zig-zag ladder. We find that there are two important similarities. Firstly, there are similarities in the ground state degeneracy. The cohomology problem for the square lattice with doubly periodic boundary conditions was solved for a large class of periodicities [21, 25]. It was found that for the zig-zag ladder there is an exponential number of zero energy states that occur in the range of fillings between $1/5$ and $1/4$. The counting of the ground states is rather non-trivial and can be formulated as a tiling problem. Secondly, there are similarities

in the spectrum. The spectrum of the zig-zag ladder was investigated and it was found that there are gapped as well as gapless sectors [19, 21]. In particular, the spectrum was found to be gapped at $1/4$ filling, and the four zero energy states are simple product states with a particle resonating on every fourth diagonal rung. This is very similar to the $1/4$ filled ground states of the two-leg triangular ladder (although in this case there are only two). For the zig-zag ladder it was found that the spectrum is also gapped at $1/5$ filling. The gapless phase was observed at intermediate fillings. In particular, $2/9$ filling seems to play an important role. We think that the ladder considered here can shed light on the physics of the zig-zag ladder. What we observe here at $1/6$ filling may be a cartoon version of what is going on in the zig-zag ladder at $2/9$ filling. A promising route could be to try to perturb the ladder considered here, in such a way that the dark states become mobile. Another possibility is to study the zig-zag ladder in the limit of zero staggering on every third site of the zig-zag chain. In this limit the spectrum bears very strong resemblances to that of the ladder studied here. In fact, it also falls apart into many sectors, some gapped, some gapless, with the gapless sectors described by (sums of) superconformal field theories with central charge $c = 1$.

5. Conclusions

In this paper, we combined numerical and analytical techniques to investigate the ground state structure of the supersymmetric model on the triangular lattice with doubly periodic boundary conditions. Previous studies showed that this system has an exponential ground state degeneracy, leading to an extensive ground state entropy [9, 36]. Furthermore, zero energy states were proven to exist between $1/7$ and $1/5$ filling [29]. Our numerical studies confirm these results. The two main results we obtain in this work for the full 2D triangular lattice are an analytic upper bound on the range of fillings for which zero energy states can exist, namely between $1/8$ and $1/4$ filling, and the numerical observation that the system typically exhibits a 2D flatband dispersion, which we believe to persist for the full 2D model.

We also studied three ladder geometries in more detail and presented a variety of new results. For the four-leg ladder we present a slightly sharper upper bound to the total number of ground states and we conjecture a sharper bound on the range of fillings for which zero energy states exist. For the three-leg ladder we find that the ground state structure is very different for odd and even lengths, L. For L even we find the total number of ground states for each particle number sector analytically by solving the cohomology problem, for odd L this result is still lacking. We do, however, present a rigorous lower bound on the cohomology, which is in perfect agreement with the numerical data, and conjecture that it is exact [35]. Furthermore, numerical computations for the ground state degeneracy in each momentum sector clearly show a flatband for L even for momenta in both the vertical and the horizontal direction. For L odd we do not observe a flatband, instead the ground states all have $p_x = 2\pi - p_y = 2\pi k/3$, with $k = 0, 1, 2$. Interestingly, many of the results for the three-leg ladder can be understood from a mapping between ground states and tilings. This is thus another example where a non-trivial relation between tilings and ground states of the supersymmetric model is observed [21, 25, 27, 29].

Finally, we discuss the full solution for the two-leg ladder. For this system the ground state degeneracy can be understood in terms of a local $\mathbb{Z}_2$ symmetry of the lattice. Furthermore, we find a mapping from the ladder to the chain such that the entire spectrum can be understood. Remarkably, in certain sectors the spectrum turns out to be gapped, in others it is gapless and in

yet other sectors we find phase separation. The continuum limit of each of the gapless sectors is shown to be described by a superconformal field theory with central charge $c = 1$. We argue that this model can shed light on the rich physics observed for the supersymmetric model on the zig-zag ladder [19, 21].

Acknowledgments

We would like to thank J Jonsson and B Nienhuis for discussions at the early stages of this work and E Berg and P Fendley for discussions on the two-leg ladder. We wish to acknowledge the SFI/HEA Irish Centre for High-End Computing (ICHEC) for the provision of computational facilities and support. LH acknowledges funding from the Netherlands Organisation for Scientific Research (NWO). DM was supported by the US Department of Energy under contract no. DE-FG02-85ER40237 and by the Science Foundation Ireland grant no. 08/RFP/PHY1462. JV was supported by the Science Foundation Ireland through the Principal Investigator Award 10/IN.1/I3013.

Appendix A. Mapping of two-leg ladder Hamiltonian to the chain Hamiltonian

In this appendix, we give some details of the computation that leads to the identification of the Hamiltonian on the two-leg ladder in the even parity sector with the Hamiltonian on the chain. Let us introduce the creation operator $\tilde{c}_i^\dagger \equiv (c_{2i-1}^\dagger + c_{2i}^\dagger)/\sqrt{2}$, which creates the $|+\rangle_i$ from the empty rung. Furthermore, we introduce the number operator $\tilde{n}_i = n_{2i-1} + n_{2i}$ and the projection operator $\tilde{P}_{\langle j\rangle} = (1-\tilde{n}_{(j-1)})(1-\tilde{n}_{(j+1)})$. Note that the latter is indeed a projection operator, because due to the nearest-neighbor exclusion $\tilde{n}_i$ only takes the values 0 or 1. When we label the L_+ even parity rungs 1 through L_+, the Hamiltonian on that part of the system reads

$$H_+ = H_{\text{kin}} + H_{\text{pot}} = \sum_{i=0}^{2L_+} \sum_{j\in\langle i\rangle} P_{\langle i\rangle} c_i^\dagger c_j P_{\langle i\rangle} + \sum_{i=0}^{2L_+} P_{\langle i\rangle}. \tag{A.1}$$

Expanding these terms, we can rewrite this Hamiltonian in terms of the operators we just introduced which are defined on a chain of L_+ sites. We first rewrite the latter term.

$$\begin{aligned}
H_{\text{pot}} &= \sum_{j=1}^{L_+} P_{\langle 2j-1\rangle} + P_{\langle 2j\rangle} \\
&= \sum_{j=1}^{L_+} [(1-n_{2j}) + (1-n_{2j-1})](1 - n_{2(j-1)-1} - n_{2(j-1)} + n_{2(j-1)-1} n_{2(j-1)}) \\
&\quad \times (1 - n_{2(j+1)-1} - n_{2(j+1)} + n_{2(j+1)-1} n_{2(j+1)}) \\
&= \sum_{j=1}^{L_+} (2 - n_{2j} - n_{2j-1})(1 - n_{2(j-1)-1} - n_{2(j-1)})(1 - n_{2(j+1)-1} - n_{2(j+1)}) \\
&= \sum_{j=1}^{L_+} (2 - \tilde{n}_j)(1 - \tilde{n}_{(j-1)})(1 - \tilde{n}_{(j+1)}) \\
&= \sum_{j=1}^{L_+} (2\tilde{P}_{\langle j\rangle} - \tilde{n}_j),
\end{aligned} \tag{A.2}$$

where we have used the fact that $n_j n_{i\,\text{next to}\,j} = 0$ for the hard-core fermions in the third and the last line. To rewrite the kinetic term we first note that

$$P_{\langle 2j\rangle} c_{2j}^\dagger = (1 - n_{2j-1})\tilde{P}_{\langle j\rangle} c_{2j}^\dagger \quad \text{and}$$
$$c_{2j} P_{\langle 2j\rangle} = c_{2j}(1 - n_{2j-1})\tilde{P}_{\langle j\rangle} = c_{2j}\tilde{P}_{\langle j\rangle},$$

where, in the last step, we use the fact that for hard-core fermions $c_{2j} n_{2j-1} = 0$. It follows that we can write the kinetic term as

$$\begin{aligned}
H_{\text{kin}} = \sum_{j=1}^{L_+} [& P_{\langle 2j\rangle} c_{2j}^\dagger c_{2j-1} P_{\langle 2j-1\rangle} + P_{\langle 2j-1\rangle} c_{2j-1}^\dagger c_{2j} P_{\langle 2j\rangle} \\
& + \sum_{i=j\pm 1} (P_{\langle 2j\rangle} c_{2j}^\dagger + P_{\langle 2j-1\rangle} c_{2j-1}^\dagger)(c_{2i-1} P_{\langle 2i-1\rangle} + c_{2i} P_{\langle 2i\rangle})] \\
= \sum_{j=1}^{L_+} [& \tilde{P}_{\langle j\rangle}(1 - n_{2j-1}) c_{2j}^\dagger c_{2j-1} \tilde{P}_{\langle j\rangle} + \tilde{P}_{\langle j\rangle}(1 - n_{2j}) c_{2j-1}^\dagger c_{2j} \tilde{P}_{\langle j\rangle} \\
& + \sum_{i=j\pm 1} (\tilde{P}_{\langle j\rangle}(1 - n_{2j-1}) c_{2j}^\dagger + \tilde{P}_{\langle j\rangle}(1 - n_{2j}) c_{2j-1}^\dagger)(c_{2i-1}\tilde{P}_{\langle i\rangle} + c_{2i}\tilde{P}_{\langle i\rangle})] \\
= \sum_{j=1}^{L_+} [& \tilde{P}_{\langle j\rangle}(c_{2j}^\dagger c_{2j-1} + c_{2j-1}^\dagger c_{2j})\tilde{P}_{\langle j\rangle} + \sum_{i=j\pm 1} \tilde{P}_{\langle j\rangle}\sqrt{2}\tilde{c}_j^\dagger \sqrt{2}\tilde{c}_i \tilde{P}_{\langle i\rangle}],
\end{aligned} \tag{A.3}$$

where in the last line we used the fact that $n_{2j-1} c_{2j}^\dagger c_{2j-1} = c_{2j}^\dagger n_{2j-1} c_{2j-1} = 0$ in the first term. In the second term we used the fact that $n_{2j} c_{2j-1}^\dagger c_{2i-1}\tilde{P}_{\langle i\rangle} = c_{2j-1}^\dagger c_{2i-1} n_{2j}\tilde{P}_{\langle i\rangle} = 0$ because $\tilde{P}_{\langle i\rangle}$ contains the term $(1 - n_{2j})$. Similarly, we have $n_{2j-1}\tilde{P}_{\langle i\rangle} = 0$. Finally, we note that $\tilde{P}_{\langle j\rangle}(c_{2j}^\dagger c_{2j-1} + c_{2j-1}^\dagger c_{2j})\tilde{P}_{\langle j\rangle}|0\rangle_j = 0$ and $\tilde{P}_{\langle j\rangle}(c_{2j}^\dagger c_{2j-1} + c_{2j-1}^\dagger c_{2j})\tilde{P}_{\langle j\rangle}|+\rangle_j = |+\rangle_j$, so we can simply replace this term by $\tilde{n}_j$.

Adding the potential and kinetic terms we obtain

$$H_+ = \sum_{j=1}^{L_+} \sum_{i=j\pm 1} 2\tilde{P}_{\langle j\rangle}\tilde{c}_j^\dagger \tilde{c}_i \tilde{P}_{\langle i\rangle} + \sum_{j=1}^{L_+} 2\tilde{P}_{\langle j\rangle} = 2H_{\text{chain}}. \tag{A.4}$$

Appendix B. Numerical data on ground state degeneracy

B.1. Size $3 \times L$, *L odd*

We show the ground state degeneracy for the three-leg ladder of odd length L for the non-trivial sectors with particle number $f = (L \pm 1)/2$ and momenta $p_x = 2\pi - p_y = 2\pi k/3$, with $k = 0, 1, 2$. We also indicate the total number of zero energy states, N_{gs}, and the Witten index, W. We present data for $L = 3, \ldots, 21$.

3×3

$N_{\mathrm{gs}} = 2, W = -2$

(f,k)	0	1	2
1	0	1	1
2	0	0	0

3×5

$N_{\mathrm{gs}} = 1, W = 1$

(f,k)	0	1	2
2	1	0	0
3	0	0	0

3×7

$N_{\mathrm{gs}} = 1, W = 1$

(f,k)	0	1	2
3	0	0	0
4	1	0	0

3×9

$N_{\mathrm{gs}} = 8, W = -2$

(f,k)	0	1	2
4	1	1	1
5	1	2	2

3×11

$N_{\mathrm{gs}} = 3, W = 1$

(f,k)	0	1	2
5	1	0	0
6	2	0	0

3×13

$N_{\mathrm{gs}} = 5, W = 1$

(f,k)	0	1	2
6	3	0	0
7	2	0	0

3×15

$N_{\mathrm{gs}} = 24, W = -2$

(f,k)	0	1	2
7	3	5	5
8	3	4	4

3×17

$N_{\mathrm{gs}} = 15, W = 1$

(f,k)	0	1	2
8	8	0	0
9	7	0	0

3×19

$N_{\mathrm{gs}} = 23, W = 1$

(f,k)	0	1	2
9	11	0	0
10	12	0	0

3×21

$N_{\mathrm{gs}} = 132, W = -2$

(f,k)	0	1	2
10	21	22	22
11	21	23	23

B.2. Size $3 \times L$, *L even*

For the three-leg ladder the total number of ground states is understood analytically as explained in section 3.2. The degeneracy per momentum sector can also be understood from the mapping between cohomology elements to tilings up to the mismatch given in (3.10). For this reason we do not give all the numerical results here, instead we explain the momentum assignment derived from the tilings for one example. We consider the three-leg ladder of length $L = 12$. The numerical computation of the ground state degeneracy per momentum sector reveals the following pattern.

3×12	
$N_{\rm gs} = 130, W = 130$	
(k_x, k_y)	0 1 2
0	4 3 3
1	3 4 4
2	3 4 3
3	6 4 4
4	3 3 3
5	3 4 4
6	4 3 3
7	3 4 4
8	3 3 3
9	6 4 4
10	3 3 4
11	3 4 4

We now reconstruct this pattern via the tiling correspondence. One example of a tiling is given figure 9. Let us refer to this tiling as RRGGRG, which stand for the sequence of red (R) and green (G) tiles. The unit cell of this tiling contains 36 sites and thus corresponds to 36 ground states. We write the eigenvalues of translations along $\vec{u} = (0, M)$ and $\vec{v} = (N, 0)$ as $t_y = \mathrm{e}^{2\pi \imath k_y/M}$ and $t_x = \mathrm{e}^{2\pi \imath k_x/N}$, respectively. It follows that the tiling RRGGRG has eigenvalues $t_x^{12} = 1$ and $t_y^3 = 1$. Therefore the 36 ground states are distributed evenly over the 36 momentum sectors. This is also true for the ground states corresponding to the tilings RRRGGG and GGRRGR. We thus have so far accounted for three ground states in each momentum sector. The tiling with all red tiles and the tiling with all green tiles each have a unit cell of six sites. They each correspond to six ground states and taking into account the fermionic character of the particles we find the following for the translation eigenvalues. The red tiling has eigenvalues $t_x^2 t_y = -1$ and $t_y^3 = 1$ and the green tiling has $t_x^2 = -1$ and $t_y^3 = 1$. The momentum assignment is thus $(k_x, k_y) = (3, 0), (9, 0), (1, 1), (7, 1), (5, 2), (11, 2)$ for the red tiling and $(k_x, k_y) = (3, k), (9, k)$ with $k = 0, 1, 2$ for the green tiling. Finally, there is a tiling which has red and green tiles alternating leading to a unit cell, RG, of 12 sites. The translation eigenvalues are $t_x^4 t_y = 1$ and $t_y^3 = 1$, leading to the momentum assignment: $(k_x, k_y) = (3n - k \bmod 12, k)$ with $k = 0, 1, 2$ and $n = 0, 3, 6, 9$. We readily check that this argument correctly reproduces the degeneracies in all momentum sectors with the exception of the sectors $p_x = 2\pi - p_y = 2\pi k/3$ with $k = 1, 2$. In these two sectors the degeneracy is 3, whereas the tiling argument gives 4. It follows that of the 12 tilings of type RG only 10 correspond to ground states.

B.3. Size $4 \times L$

We show the ground state degeneracy for the four-leg ladder of length L for the non-trivial sectors with particle number f and momenta $(p_x, p_y) = (2\pi k_x/L, 2\pi k_y/4)$. We also indicate the total number of zero energy states, $N_{\rm gs}$, and the Witten index, W. We present data for $L = 4, \ldots, 12$.

4×4

$N_{\rm gs} = 23, W = -23$

$f = 3$

(k_x, k_y)	0	1	2	3
0	2	1	1	1
1	1	1	2	2
2	1	2	1	2
3	1	2	2	1

4×5

$N_{\rm gs} = 11, W = 11$

$f = 4$

(k_x, k_y)	0	1	2	3
0	2	0	1	0
1	1	0	1	0
2	1	0	1	0
3	1	0	1	0
4	1	0	1	0

4×6

$N_{\rm gs} = 29, W = 25$

$f = 4$

(k_x, k_y)	0	1	2	3
0	2	1	3	1
1	1	1	0	1
2	2	0	3	0
3	1	1	1	1
4	2	0	3	0
5	1	1	0	1

$f = 5$

(k_x, k_y)	0	1	2	3
0	0	0	1	0
1	0	0	0	0
2	0	0	0	0
3	0	0	1	0
4	0	0	0	0
5	0	0	0	0

4×7

$N_{\rm gs} = 69, W = -69$

$f = 5$

(k_x, k_y)	0	1	2	3
0	2	2	3	2
1	3	2	3	2
2	3	2	3	2
3	3	2	3	2
4	3	2	3	2
5	3	2	3	2
6	3	2	3	2

4×8

$N_{\rm gs} = 193, W = 193$

$f = 6$

(k_x, k_y)	0	1	2	3
0	4	7	4	7
1	6	8	6	7
2	4	7	4	6
3	6	7	6	8
4	5	6	4	6
5	6	8	6	7
6	4	6	4	7
7	6	7	6	8

4×9

$N_{\rm gs} = 151, W = -29$

$f = 6$

(k_x, k_y)	0	1	2	3
0	2	3	1	3
1	1	2	1	2
2	1	2	1	2
3	1	3	1	3
4	1	2	1	2
5	1	2	1	2
6	1	3	1	3
7	1	2	1	2
8	1	2	1	2

$f = 7$

(k_x, k_y)	0	1	2	3
0	2	3	2	3
1	2	3	2	3
2	2	3	2	3
3	2	3	2	3
4	2	3	2	3
5	2	3	2	3
6	2	3	2	3
7	2	3	2	3
8	2	3	2	3

4×10

$N_{\rm gs} = 293, W = -279$

$f = 7$		$f = 8$	
(k_x, k_y)	0 1 2 3	(k_x, k_y)	0 1 2 3
0	5 8 7 8	0	1 0 1 0
1	7 8 6 8	1	0 0 0 0
2	5 9 5 9	2	1 0 0 0
3	7 8 6 8	3	0 0 0 0
4	5 9 5 9	4	1 0 0 0
5	7 8 7 8	5	0 0 1 0
6	5 9 5 9	6	1 0 0 0
7	7 8 6 8	7	0 0 0 0
8	5 9 5 9	8	1 0 0 0
9	7 8 6 8	9	0 0 0 0

4×11

$N_{\rm gs} = 859, W = 859$

$f = 8$	
(k_x, k_y)	0 1 2 3
0	22 18 21 18
1	21 18 21 18
2	21 18 21 18
3	21 18 21 18
4	21 18 21 18
5	21 18 21 18
6	21 18 21 18
7	21 18 21 18
8	21 18 21 18
9	21 18 21 18
10	21 18 21 18

4×12

$N_{\rm gs} = 1439, W = -1295$

$f = 8$		$f = 9$	
(k_x, k_y)	0 1 2 3	(k_x, k_y)	0 1 2 3
0	6 0 3 0	0	32 27 31 27
1	1 1 2 0	1	30 26 30 26
2	2 1 3 1	2	30 26 30 26
3	1 0 2 1	3	31 27 32 28
4	6 0 3 0	4	30 26 30 26
5	1 1 2 0	5	30 26 30 26
6	2 1 3 1	6	31 28 31 28
7	1 0 2 1	7	30 26 30 26
8	6 0 3 0	8	30 26 30 26
9	1 1 2 0	9	31 28 32 27
10	2 1 3 1	10	30 26 30 26
11	1 0 2 1	11	30 26 30 26

B.4. Size $5 \times L$

We show the ground state degeneracy for the five-leg ladder of length L for the non-trivial sectors with particle number f and momenta $(p_x, p_y) = (2\pi k_x/L, 2\pi k_y/5)$. We also indicate the total number of zero energy states, $N_{\rm gs}$, and the Witten index, W. We present data for $L = 5, 6, 7$.

5×5

$N_{\rm gs} = 66, W = 36$

$f = 4$		$f = 5$	
(k_x, k_y)	0 1 2 3 4	(k_x, k_y)	0 1 2 3 4
0	3 2 2 2 2	0	3 0 0 0 0
1	2 2 2 2 2	1	0 0 1 1 1
2	2 2 2 2 2	2	0 1 0 1 1
3	2 2 2 2 2	3	0 1 1 0 1
4	2 2 2 2 2	4	0 1 1 1 0

5×6

$N_{\rm gs} = 55, W = -49$

$f = 5$		$f = 6$	
(k_x, k_y)	0 1 2 3 4	(k_x, k_y)	0 1 2 3 4
0	1 1 1 1 1	0	1 0 0 0 0
1	2 2 2 2 2	1	0 0 0 0 0
2	2 2 2 2 2	2	0 0 0 0 0
3	3 1 1 1 1	3	2 0 0 0 0
4	2 2 2 2 2	4	0 0 0 0 0
5	2 2 2 2 2	5	0 0 0 0 0

5×7

$N_{\rm gs} = 215, W = 211$

$f = 6$						$f = 7$					
(k_x, k_y)	0	1	2	3	4	(k_x, k_y)	0	1	2	3	4
0	9	6	6	6	6	0	2	0	0	0	0
1	6	6	6	6	6	1	0	0	0	0	0
2	6	6	6	6	6	2	0	0	0	0	0
3	6	6	6	6	6	3	0	0	0	0	0
4	6	6	6	6	6	4	0	0	0	0	0
5	6	6	6	6	6	5	0	0	0	0	0
6	6	6	6	6	6	6	0	0	0	0	0

B.5. Size $6 \times L$

We show the ground state degeneracy for the six-leg ladder of length L for the non-trivial sectors with particle number f and momenta $(p_x, p_y) = (2\pi k_x/L, 2\pi k_y/6)$. We also indicate the total number of zero energy states, $N_{\rm gs}$, and the Witten index, W. We present data for $L = 6, 7, 8, 9$.

6×6

$N_{\rm gs} = 184, W = -102$

$f = 6$							$f = 7$						
(k_x, k_y)	0	1	2	3	4	5	(k_x, k_y)	0	1	2	3	4	5
0	2	2	0	5	0	2	0	6	4	4	5	4	4
1	2	2	0	1	1	0	1	4	4	3	4	4	3
2	0	0	0	1	0	1	2	4	3	4	4	4	4
3	5	1	1	5	1	1	3	5	4	4	5	4	4
4	0	1	0	1	0	0	4	4	4	4	4	4	3
5	2	0	1	1	0	2	5	4	3	4	4	3	4

6×7

$N_{\rm gs} = 269, W = -13$

$f = 7$							$f = 8$						
(k_x, k_y)	0	1	2	3	4	5	(k_x, k_y)	0	1	2	3	4	5
0	4	3	3	5	3	3	0	4	3	3	4	3	3
1	4	3	3	4	3	3	1	3	3	3	3	3	3
2	4	3	3	4	3	3	2	3	3	3	3	3	3
3	4	3	3	4	3	3	3	3	3	3	3	3	3
4	4	3	3	4	3	3	4	3	3	3	3	3	3
5	4	3	3	4	3	3	5	3	3	3	3	3	3
6	4	3	3	4	3	3	6	3	3	3	3	3	3

6×8

$N_{\rm gs} = 619, W = -415$

$f = 8$		$f = 9$	
(k_x, k_y)	0 1 2 3 4 5	(k_x, k_y)	0 1 2 3 4 5
0	5 2 4 3 4 2	0	13 10 10 13 10 10
1	2 1 2 1 2 1	1	12 10 10 12 10 10
2	2 2 2 2 2 2	2	11 10 10 12 10 10
3	2 1 2 1 2 1	3	12 10 10 12 10 10
4	7 1 5 3 5 1	4	15 10 10 14 10 10
5	2 1 2 1 2 1	5	12 10 10 12 10 10
6	2 2 2 2 2 2	6	11 10 10 12 10 10
7	2 1 2 1 2 1	7	12 10 10 12 10 10

6×9

$N_{\rm gs} = 1926, W = 1462$

$f = 9$		$f = 10$	
(k_x, k_y)	0 1 2 3 4 5	(k_x, k_y)	0 1 2 3 4 5
0	9 3 3 9 3 3	0	33 31 31 33 31 31
1	4 5 3 4 5 3	1	32 31 31 32 31 31
2	4 3 5 4 3 5	2	32 31 31 32 31 31
3	7 4 4 7 3 4	3	32 32 31 32 30 31
4	4 5 3 4 5 3	4	32 31 31 32 31 31
5	4 3 5 4 3 5	5	32 31 31 32 31 31
6	7 4 3 7 4 4	6	32 31 30 32 31 32
7	4 5 3 4 5 3	7	32 31 31 32 31 31
8	4 3 5 4 3 5	8	32 31 31 32 31 31

B.6. Size $7 \times L$

We show the ground state degeneracy for the system of size 7×7 for the non-trivial sectors with particle number f and momenta $(p_x, p_y) = (2\pi k_x/7, 2\pi k_y/7)$. We also indicate the total number of zero energy states, $N_{\rm gs}$, and the Witten index, W.

7×7

$N_{\rm gs} = 1193, W = -797$

$f = 7$		$f = 8$		$f = 9$	
(k_x, k_y)	0 1 2 3 4 5 6	(k_x, k_y)	0 1 2 3 4 5 6	(k_x, k_y)	0 1 2 3 4 5 6
0	2 0 0 0 0 0 0	0	6 4 4 4 4 4 4	0	21 20 20 20 20 20 20
1	0 0 0 1 0 1 0	1	4 4 4 4 4 4 4	1	20 20 20 20 20 20 20
2	0 0 0 1 0 0 1	2	4 4 4 4 4 4 4	2	20 20 20 20 20 20 20
3	0 1 1 0 0 0 0	3	4 4 4 4 4 4 4	3	20 20 20 20 20 20 20
4	0 0 0 0 0 1 1	4	4 4 4 4 4 4 4	4	20 20 20 20 20 20 20
5	0 1 0 0 1 0 0	5	4 4 4 4 4 4 4	5	20 20 20 20 20 20 20
6	0 0 1 0 1 0 0	6	4 4 4 4 4 4 4	6	20 20 20 20 20 20 20

References

[1] http://www.grycap.upv.es/slepc/documentation/manual.htm
[2] Adamaszek M 2011 Special cycles in independence complexes and superfrustration in some lattices arXiv:1109.4914v2
[3] Bagger J, Duplij S and Siegel W (ed) 2003 *Concise Encyclopedia of SUPERSYMMETRY and Noncommutative Structures in Mathematics and Physics* (Dordrecht: Kluwer)
[4] Baxter R J 2011 Hard squares for $z = -1$ *Ann. Comb.* **15** 185–95
[5] Beccaria M and De Angelis G F 2005 Exact ground state and finite size scaling in a supersymmetric lattice model *Phys. Rev. Lett.* **94** 100401
[6] Bott R and Tu L W 1982 *Differential Forms in Algebraic Topology* (New York: Springer)
[7] Bousquet-Melou M, Linusson S and Nevo E 2008 On the independence complex of square grids *J. Algebr. Comb.* **27** 423–50
[8] Csorba P 2009 Subdivision Yields Alexander Duality on Independence Complexes *Electron. J. Comb.* **16** #R11
[9] Engström A 2009 Upper bounds on the Witten index for supersymmetric lattice models by discrete Morse theory *Eur. J. Comb.* **30** 429–38
[10] Fendley P 2007 private communication
[11] Fendley P and Hagendorf C 2010 Exact and simple results for the XYZ and strongly interacting fermion chains *J. Phys. A: Math. Theor.* **43** 402004
[12] Fendley P and Hagendorf C 2011 Ground-state properties of a supersymmetric fermion chain *J. Stat. Mech.* **1102** P02014
[13] Fendley P, Nienhuis B and Schoutens K 2003 Lattice fermion models with supersymmetry *J. Phys. A: Math. Gen.* **36** 12399
[14] Fendley P and Schoutens K 2005 Exact results for strongly correlated fermions in $2+1$ dimensions *Phys. Rev. Lett.* **95** 046403
[15] Fendley P, Schoutens K and de Boer J 2003 Lattice models with $\mathcal{N} = 2$ supersymmetry *Phys. Rev. Lett.* **90** 120402
[16] Fendley P, Schoutens K and van Eerten H 2005 Hard squares at negative activity *J. Phys. A: Math. Gen.* **38** 315
[17] Galanakis D, Papanikolaou S and Henley C 2012 Supersymmetry in strongly correlated fermion models *APS March Meeting* **57** X8.00011
[18] Hagendorf C and Fendley P 2012 The eight-vertex model and lattice supersymmetry *J. Stat. Phys.* **146** 1122
[19] Huijse L 2010 A supersymmetric model for lattice fermions *PhD Thesis* University of Amsterdam
[20] Huijse L 2011 Detailed analysis of the continuum limit of a supersymmetric lattice model in 1D *J. Stat. Mech.* **1104** P04004
[21] Huijse L, Halverson J, Fendley P and Schoutens K 2008 Charge frustration and quantum criticality for strongly correlated fermions *Phys. Rev. Lett.* **101** 146406
[22] Huijse L, Moran N, Vala J and Schoutens K 2011 Exact ground states of a staggered supersymmetric model for lattice fermions *Phys. Rev.* B **84** 115124
[23] Huijse L and Schoutens K 2008 Superfrustration of charge degrees of freedom *Euro. Phys. J.* B **64** 543–50
[24] Huijse L and Schoutens K 2010 *Quantum Phases of Supersymmetric Lattice Models* ed P Exner *XVITH Int. Congr. Math. Phys*. (World Scientific), pp 635–9
[25] Huijse L and Schoutens K 2010 Supersymmetry, lattice fermions, independence complexes and cohomology theory *Adv. Theor. Math. Phys.* **14** 643–94
[26] Jonsson J 2006 Hard squares on grids with diagonal boundary conditions *Preprint*
[27] Jonsson J 2006 Hard squares with negative activity and rhombus tilings of the plane *Electron. J. Comb.* **13** # R67

[28] Jonsson J 2009 Hard squares with negative activity on cylinders with odd circumference *Electron. J. Comb.* **16** #R5
[29] Jonsson J 2010 Certain homology cycles of the independence complex of grids *Discrete Comput. Geom.* **43** 927–50
[30] Lee T Y, Li T Y and Zeng Z 2009 A rank-revealing method with updating, downdating and applications part ii *SIAM J. Matrix Anal. Appl.* **31** 503–25
[31] Li T Y and Zeng Z. 2005 A rank-revealing method with updating, downdating and applications *SIAM J. Matrix Anal. Appl.* **26** 918–46
[32] Moran N, Kells G and Vala J 2011 Diagonalisation of quantum observables on regular lattices and general graphs *Comput. Phys. Commun.* **182** 1083–92
[33] Pollmann F, Betouras J J, Shtengel K and Fulde P 2006 Correlated fermions on a checkerboard lattice *Phys. Rev. Lett.* **97** 170407
[34] Pollmann F, Betouras J J, Shtengel K and Fulde P 2011 Fermionic quantum dimer and fully packed loop models on the square lattice *Phys. Rev.* B **83** 155117
[35] Schoutens K and Huijse L 2012 in preparation
[36] van Eerten H 2005 Extensive ground state entropy in supersymmetric lattice models *J. Math. Phys.* **46** 123302
[37] Witten E 1982 Constraints on supersymmetry breaking *Nucl. Phys.* B **202** 253–316